UCRL-10426

University of California

Ernest O. Lawrence Radiation Laboratory

TWO-WEEK LOAN COPY

This is a Library Circulating Copy which may be borrowed for two weeks. For a personal retention copy, call Tech. Info. Division, Ext. 5545

THE LOW-TEMPERATURE HEAT CAPACITY OF TIN AND INDIUM

Berkeley, California

DISCLAIMER

This document was prepared as an account of work sponsored by the United States Government. While this document is believed to contain correct information, neither the United States Government nor any agency thereof, nor the Regents of the University of California, nor any of their employees, makes any warranty, express or implied, or assumes any legal responsibility for the accuracy, completeness, or usefulness of any information, apparatus, product, or process disclosed, or represents that its use would not infringe privately owned rights. Reference herein to any specific commercial product, process, or service by its trade name, trademark, manufacturer, or otherwise, does not necessarily constitute or imply its endorsement, recommendation, or favoring by the United States Government or any agency thereof, or the Regents of the University of California. The views and opinions of authors expressed herein do not necessarily state or reflect those of the United States Government or any agency thereof or the Regents of the University of California.

Research and Development

UCRL-10426
UC-4 Chemistry
TID-4500 (18th Edition)

UNIVERSITY OF CALIFORNIA

Lawrence Radiation Laboratory
Berkeley, California

Contract No. W-7405-eng-48

THE LOW-TEMPERATURE HEAT CAPACITY OF TIN AND INDIUM

HARRY ROGER O'NEAL

(Ph.D. Thesis)

January 1963

Printed in USA. Price $1.75. Available from the
Office of Technical Services
U. S. Department of Commerce
Washington 25, D.C.

THE LOW-TEMPERATURE HEAT CAPACITY OF TIN AND INDIUM

CONTENTS

ABSTRACT v

I. Introduction 1

II. Experimental Aspects

A. Apparatus 5

B. Procedures 9

C. Preliminary Experiments 11

D. Discussion of Errors 21

III. Results

A. Indium 26

B. Tin 40

IV. DISCUSSION

A. Nuclear Quadrupole Heat Capacity 48

B. Lattice Heat Capacity 50

C. Electronic Heat Capacity 58

APPENDIX 60

ACKNOWLEDGMENTS 62

REFERENCES 63

THE LOW-TEMPERATURE HEAT CAPACITY OF TIN AND INDIUM

Harry Roger O'Neal

Lawrence Radiation Laboratory
University of California
Berkeley, California

January 1963

ABSTRACT

The heat capacity of indium was measured from 0.08°K to 4.2°K, and that of tin from 0.09°K to 1.2°K. The results on indium show that below about 0.7°K the total superconducting-state heat capacity is less than the normal-state lattice heat capacity alone. This result is surprising compared with analyses of the heat capacity data of a superconductor made in the usual way. However, the effect was not observed in tin. Comparisons with other pertinent experiments are made, and two proposed explanations of the effect are discussed.

I. INTRODUCTION

In measurements down to $0.35^{\circ}K$, Bryant and Keesom found that below $0.7^{\circ}K$ the superconducting-state heat capacity of indium is less than the normal-state lattice heat capacity alone.[1] More recently, Boorse, Herschfield, and Leupold have reported a similar effect in niobium,[2] although in this case interpretation of the experimental data is less clear.

In view of the importance of heat capacity effects to an understanding of superconductivity, this research was undertaken to verify and extend the measurements. It was felt that limited low-temperature behavior would yield information that would contribute to an understanding of the origin of these effects.

The heat capacity of a normal metal is usually expressed as the sum of a lattice and an electronic term:

$$C_N = C_{LN} + C_{EN},$$

$$C_{LN} = \alpha_N T^3 + \beta_N T^5 + \ldots,$$

$$C_{EN} = \frac{1}{3} \pi^2 k^2 N(E_F),$$

where k is Boltzmann's constant and $N(E_F)$ is the density of states at the Fermi surface. The coefficient α_N is related to the Debye characteristic temperature at the absolute zero θ_0 by

$$\alpha = \frac{12}{5} \pi^4 R\theta_0^{-3},$$

and is completely determined by elastic constants.

In the superconducting state we have

$$C_S = C_{ES} + C_{LS},$$

and

$$C_{LS} = \alpha_S T^3 + \beta_S T^5,$$

and we assume

$$C_{LS} = C_{LN},$$

and then

$$C_{ES} = C_S - C_{LS}.$$

Corak et al., some of whose results are discussed below in Secs. III B and IV, find from their analysis on vanadium

$$C_{ES} = \gamma\ T_C\ a \exp[-bT_C]/T.$$

This same result for the superconducting electronic heat capacity was obtained by Bardeen, Cooper, and Schrieffer in their theory of superconductivity.[3]

The results of Bryant and Keesom suggest that the assumption $C_{LN} = C_{LS}$ is wrong. On the other hand, measurements of elastic constants from which one can calculate θ_0 have been completed on several superconductors, including indium and niobium. Chandrasekhar and Rayne observed no change between normal and superconducting states in the velocity of a 10-Mc/sec sound wave, to 1 part in 2×10^4 for indium.[4] Alers and Waldorf observed small differences in the elastic moduli of lead, vanadium, and niobium;[5] however, these changes are too small, and in the wrong direction, to explain the calorimetric results.

X-ray diffraction, neutron diffraction, and Mössbauer experiments should show changes in θ_0 between normal and superconducting states. The only x-ray work available was done by Keesom and Onnes, who studied the diffraction pattern for lead above and below the transition

temperature,[6] but found no change. Wilkinson et al. observed neutron scattering for vanadium, niobium, and lead above and below the transition temperature.[7] They concluded that there is no pronounced change in the atomic lattice vibrations at the superconducting transition temperature. Neutron spectrometer measurements by Woods and Brockhouse discovered no change within 0.2% in lattice vibration frequencies, in lead, between normal and superconducting states.[8]

The Mössbauer effect, the resonant absorption of gamma rays, shows changes in θ_0 since the intensity of a Mössbauer line is proportional to the Debye-Waller factor. Only a few superconductors exhibit the Mössbauer effect, however, and of these only tin has been studied. Weidemann, Kienle, and Pobelle observed an increase in the Debye-Waller factor of about 0.4% in the superconducting state;[9] this corresponds to a small decrease in θ_0. Yagub and Hohemenser also measured tin, and concluded that the change in θ_0 could be no more than $0.76^{\circ}K$.[10]

Chester[11] and Marcus and Maxwell[12] have shown that if the similarity principle holds, the lattice heat capacity is the same in both states. The similarity principle states that the reduced critical field h is independent of isotopic mass, and that $h = H/H_0$, where H_0 is the critical field at $0^{\circ}K$.

Chester shows this, by first assuming the similarity principle, as

$$H_C = (\bar{M})^{-\alpha_\Phi} \left((\bar{M})^{\alpha} T \right). \qquad (1)$$

The free-energy difference between normal and superconducting states is

$$F_N - F_S = \frac{Hc^2 V}{8\pi}, \qquad (2)$$

and the heat capacity difference is

$$C_N - C_S = -T\left(\frac{\partial^2 F}{\partial T^2}\right)_p .$$

Inserting (1) into (2) and differentiating gives us

$$C_N - C_S \sim (\overline{M})^{-\alpha}\, \psi(\,(\overline{M})^{\alpha}\ T), \qquad (3)$$

where symbol $\sim$ indicates the functional dependence of $C_N - C_S$ on $\overline{M}$ and T. Any term in C_N having a different functional dependence on $\overline{M}$ and T must be canceled by an equal term in C_S. Since it can be shown that C_{LN} depends on mass and temperature only through the variable MT^2, the lattice heat capacity must be the same in the two states.

Marcus and Maxwell arrived at the same conclusion by starting from the two-fluid model. They assumed the lattice free energy to be the same in the two states, and then derived the similarity relations. These authors show that if the lattice free energy is not the same, the critical field curve could not be written in purely reduced form. And since deviations from the similarity principle have not been observed, they conclude that the lattice free energy must be the same in normal and superconducting states.

II. EXPERIMENTAL ASPECTS

A. Apparatus

Figure 1 shows the apparatus set up for an experiment below $1^{\circ}K$, using the technique of adiabatic demagnetization of a paramagnetic salt. This apparatus is similar to that described by Phillips[13] and by Lien[14]. The apparatus shown in Fig. 1 differs, however, in two major respects from the earlier version. First, it uses two different paramagnetic salts, one as cooling salt and the other as thermometer. Second, superconducting niobium coils are used to destroy superconductivity, both in the superconducting switch and in the sample.

In choosing a paramagnetic salt for cooling, one wants a salt having considerable entropy in zero field at $1^{\circ}K$ which can be removed by application of a magnetic field of, in our case, 6000 gauss. Such a salt can be cooled to a temperature of the order of $\Delta E/k$, where ΔE is the energy level splitting of the salt, and k is Boltzmann's constant. Experimentally, it is advantageous to work near $T \approx \Delta E/k$, since here the heat capacity is at a maximum and the heat leak into the system causes least warming. However, if one determines the temperature from susceptibility measurements on this same salt, he will want to work at higher temperatures, since the susceptibility is not simply related to the temperature near $\Delta E/k$.

The temperature-susceptibility relationship has been determined in the 1-to-4 $^{\circ}K$ region where the temperature is known in terms of the vapor pressure of liquid helium. The magnetic temperature T^* is defined by

$$T^* = \frac{C}{X} , \qquad (1)$$

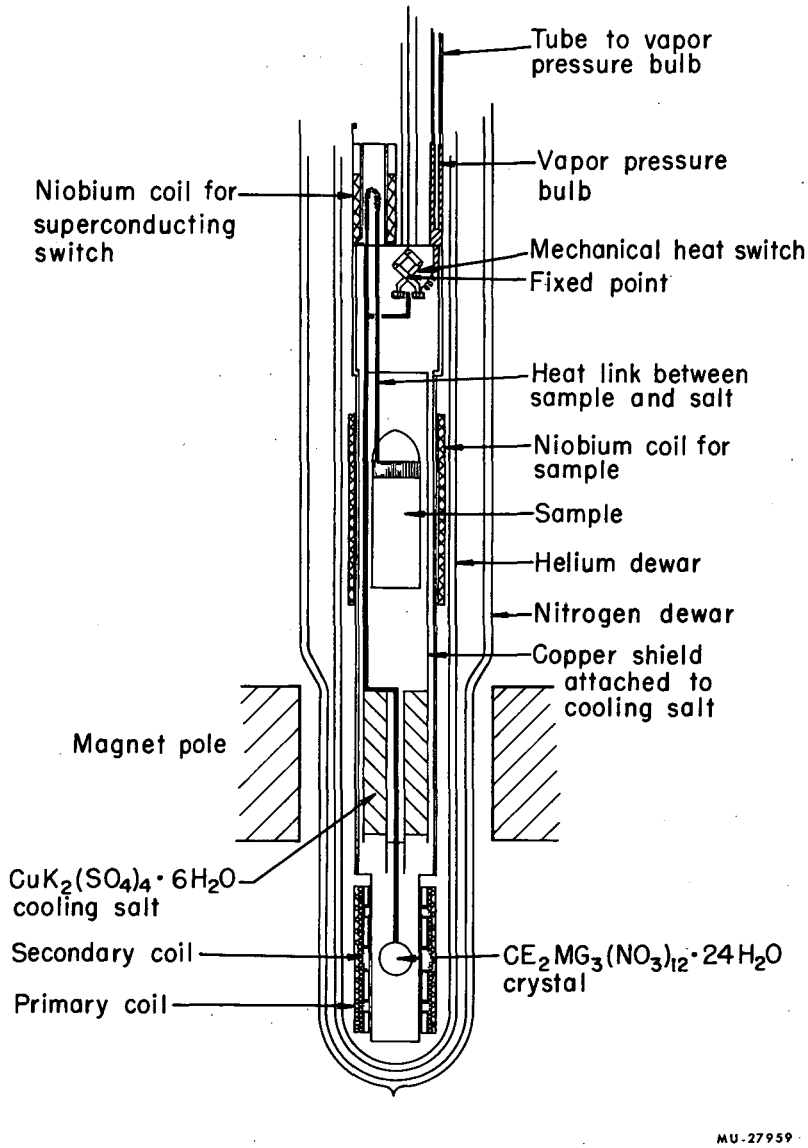

Fig. 1. Schematic diagram of the apparatus.

where C is the Curie constant and X the magnetic susceptibility. For the salts useful in temperature measurements, X follows a Curie-Weiss law between 1 and 4 ^{o}K, i.e.,

$$T^{*} = T + \Delta ,$$

where Δ is the Weiss constant and T is the thermodynamic temperature. Constants C and Δ are thus determined from the measurements on X and T in the helium region, and one can then use Eq. (1) to calculate temperatures below $1^{o}K$.

Due, then, to the unsuitability of a single paramagnetic salt to serve as both coolant and thermometer in the same temperature region, it was decided in this apparatus to employ two paramagnetic salts: $CuK_2(SO_4)_3 \cdot 6H_2O$ was retained as the cooling salt, since temperature well below $0.1^{o}K$ can be obtained with a magnetic field of only 6000 gauss. To provide rapid thermal equilibrium within the salt, a slurry of the powdered salt, its saturated solution, and glycerol as described by N. Kurti,[15] was used. As a thermometer, $Ce_2Mg_3(NO_3)_{12} \cdot 24H_2O$ was used.

Daniels and Robinson found no difference between magnetic and thermodynamic temperatures down to $0.006^{o}K$.[16] Comparisons of this type are subject to considerable experimental error, but their results certainly indicate that T and T^{*} may be taken as identical at temperatures near $0.1^{o}K$. This conclusion is further suggested by the small internal fields acting on the magnetic ions. Since the spin is $S = \frac{1}{2}$, the salt has no Stark splitting. The experimental heat capacity can be accounted for by considering the magnetic dipole interactions only,[17] implying that the exchange interactions are small.

As shown in Fig. 1, a spherical specimen of cesium magnesium nitrate was used. For a spherical sample containing free magnetic ions, the Weiss constant is zero. The spherical specimen was made by cutting two single crystals into hemispheres and gluing these to the opposite sides of a 0.005-in.-thick piece of copper foil forming the thermal link to the sample. G.E. 7031 varnish was used to glue the salt to the copper. The copper foil was hard-soldered to a heavy copper wire whose other end was connected to the superconducting switch. At its midpoint, the copper wire was hard-soldered to the copper potassium sulfate container. Arranged in this way, the sample and the $CeMgNO_3$ are in good thermal contact when the superconducting switch is closed.

An advantage of the two-salt system is that when thermal equilibrium is disturbed at temperatures near $0.1^{\circ}K$, equilibrium between the magnetic thermometer and the sample is regained in a few minutes, compared with an hour in the earlier apparatus. This is true even though temperature inhomogeneities still exist within the cooling salt, since our interest is only that equilibrium between the magnetic thermometer and sample be established.

As mentioned above, the copper coils in the nitrogen bath used by Phillips and Lien were replaced by niobium coils in the helium bath. The niobium coil controlling the superconducting switch allows one to make measurements to lower temperatures. This is because the smaller-diameter niobium coil is designed to produce a negligible field at the sample, thus reducing eddy-current heating when the field is turned off.

The niobium coil for applying a magnetic field to the sample is also a distinct improvement. The copper coil in the nitrogen bath made it boil vigorously, causing the sample to vibrate with a consequent energy

input. The copper coil for the superconducting switch had also caused the sample to vibrate during calibration, thus warming the sample and setting up temperature gradients between the sample and the magnetic thermometer. By using niobium coils, one clearly eliminates these difficulties.

The niobium coils, however, have one disadvantage: if the critical field is exceeded, a flux of a few gauss remains frozen in the coil after the current is turned off. This problem is discussed below in connection with the heat-capacity results on superconducting tin and indium.

B. Procedures

As mentioned at the beginning of the previous section, this apparatus is quite similar to that described by Lien[13] and by Phillips.[12] This is even truer of procedures and instrumentation, which are only briefly discussed here. The interested reader is referred to the detailed descriptions given by Lien.

The apparatus is slowly cooled from room to nitrogen temperatures by using hydrogen exchange gas. When cooled to $78^{\circ}K$, liquid hydrogen is put into the helium Dewar and hydrogen exchange gas cools the sample to $20^{\circ}K$. The hydrogen exchange gas is then pumped out to a pressure of the order 10^{-5} mm Hg, the liquid hydrogen is boiled out of the helium Dewar with an induction heater, and liquid helium is put into the Dewar. (The apparatus is precooled with hydrogen to conserve liquid helium.) The mechanical heat switch allows the sample to cool, in the absence of exchange gas, to $4.2^{\circ}K$.

A large Kinney pump allows us to pump the helium bath to 1.1°K. Seven or eight magnetic-susceptibility- temperature calibration points are made between 1.1 and 4.2 °K. The copper potassium sulfate is demagnetized from 1.1°K. At least two demagnetizations are required for each heat-capacity experiment, the first to calibrate the carbon resistance thermometer against the paramagnetic salt, and the second for the actual measurement of the heat capacities.

The susceptibility measurements are made on an ac bridge of the type described by Erikson et al.,[8] and the resistance of the carbon thermometer R is determined potentiometrically. The temperature-resistance calibration points are fitted to an equation of the form

$$\frac{1}{T} = C_0 + C_1 R + C_2 R^2 + C_3 R^3 + C_4 R^4. \qquad (3)$$

The fit is generally better than 1% in T. For each calibration point, then, one has an observed temperature (from the susceptibility measurements), and a calculated T from the above equation. Their fractional difference is plotted as a function of calculated temperature and a smooth curve is drawn through the point. The curve, called the "difference plot", is used to correct the temperatures calculated from Eq. (3) for the initial and final R's of each heat-capacity point.

The heat input for each heat-capacity point is determined by passing a measured current through a measured resistance (in intimate thermal contact with the sample) for a measured period of time. This amount of heat is determined to better than 0.1%.

C. Preliminary Experiments

1. Copper

The first substance measured in the new apparatus was copper. Copper has been run by a number of investigators above and below $1^{\circ}K$. The measurement of its heat capacity was undertaken as a check on the new apparatus. The 900-gram sample (99.999% pure, American Smelting and Refining Company, South Plainfield, New Jersey) had been recently annealed in vacuum for several hours at $600^{\circ}C$.

A plot of C/T vs T^2 is shown in Fig. 2, and the heat capacities are listed in Table I. The best fit to the data is given by

$$C = 0.702\ T + 0.0482\ T^3 \text{ millijoules/mole-deg.}$$

Since the lattice heat capacity is quite small below $1^{\circ}K$, the T^3 coefficient is that determined by Phillips from an experiment above $1^{\circ}K$ on the same sample.[19] The line shown in the figure is that determined here. Table II compares other recent work on heat capacity in copper.

As seen from Fig. 2, the lowest temperature points are somewhat high, as much as 2%. At $0.13^{\circ}K$ the average point is 1.5% lighter. This systematic deviation could be associated either with the temperature scale or with "addenda" corrections. These possibilities are discussed in more detail in the next section.

2. KBr

Since KBr would be expected to have only a T^3 heat capacity below $1^{\circ}K$, it was measured as a further check on the apparatus. Its heat capacity was of the order of 1% of that of typical normal metal at $0.1^{\circ}K$,

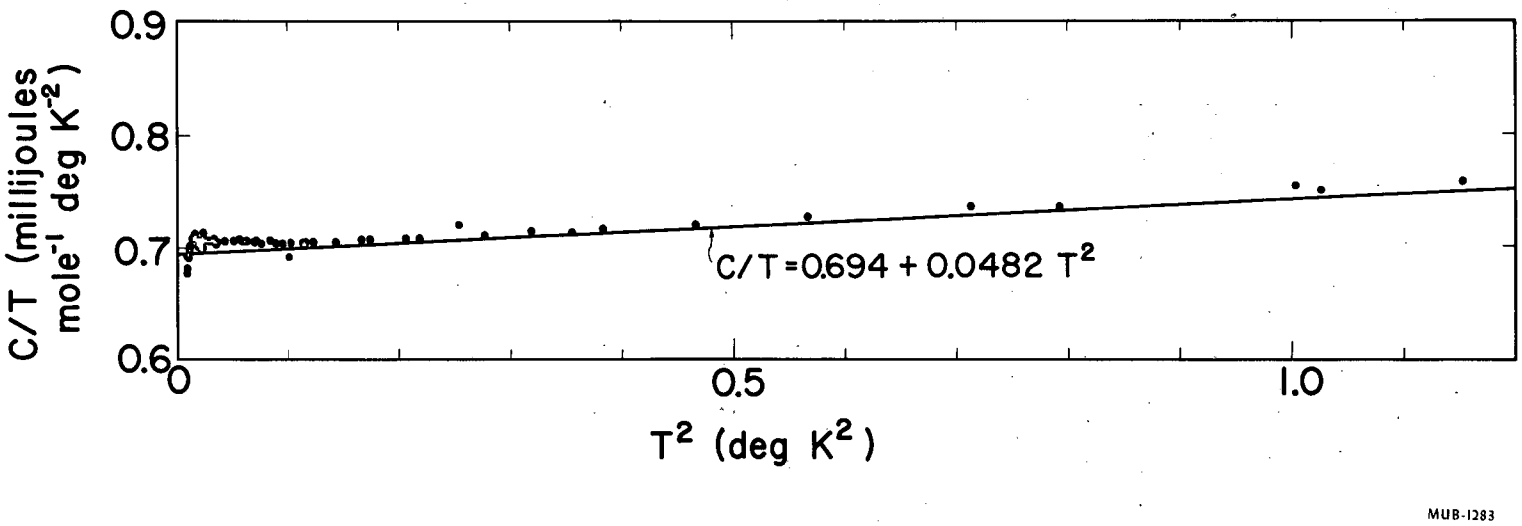

Fig. 2. The heat capacity of copper. The line is an extrapolation from measurements above 1°K on the same sample.

Table I. Heat capacity of copper.

T (^{o}K)	C (mJ/mole-deg)	T (^{o}K)	C (mJ/mole-deg)
.1074	.07494	.1672	.1182
.1171	.08297	.1852	.1311
.1266	.09025	.1389	.09749
.09731	.06641	.1546	.1103
.1078	.07539	.1709	.1206
.1190	.08445	.1885	.1325
.09656	.06534	.2072	.1462
.1020	.07046	.2274	.1604
.1077	.07549	.2516	.1775
.1276	.09093	.2763	.1946
.1166	.08269	.2392	.1689
.1507	.1054	.2637	.1860
.1065	.07420	.2898	.2046
.1187	.08431	.3203	.2257
.1321	.09416	.3523	.2483
.1451	.1025	.3085	.2173
.1586	.1123	.3426	.2414
.1735	.1224	.3780	.2665
.1911	.1348	.4171	.2949
.2118	.1495	.4085	.2888
.2368	.1675	.4540	.3215
.2661	.1878	.5035	.3623

Table I (continued)

T (^{o}K)	C (mJ/mole-deg)	T (^{o}K)	C (mJ/mole-deg)
.2991	.2106	.5652	.4037
.3370	.2376	.4678	.3312
.3804	.2681	.5264	.3742
.1004	.06947	.5956	.4250
.1388	.09809	.6187	.4429
.1302	.09231	.6825	.4916
.1500	.1047	.7528	.5470
.8444	.6216	1.0992	.8448
.8902	.6540	1.0065	.7593
1.0129	.7597	1.0736	.8149

Table II. Recent heat capacity results on copper.

	γ	α	Purity (%)
Phillips, N. E.[a]	0.694	0.0482	99.999
Kneip, G.[b]	0.698	0.0482	99.999
Rayne, J.[c]	0.686	0.0473	99.999
Corak et al.[d]	0.688	0.0478	99.999
Ahlers, G.[e]	0.704	0.0478	99.999
du Chaterier and de Nobel	0.721	0.0500	99.9999
Giffel, Vest, Smith[g]	0.691	0.0486	99.99
Manchester, F. D.[h]	0.696	0.0478	99.999
Ramanathan and Srinvason[i]	0.720	0.0523	--
Franck, Manchester, Martin[j]	0.690	0.478	99.999
This work	0.702	--	99.999

[a] Private communication.
[b] Private communication.
[c] Australian J. Phys. 9, 189 (1956).
[d] Phys. Rev. 98, 1699 (1955).
[e] Private communication.
[f] Phys. 28, 181 (1962).
[g] J. Chem. Phys. 27, 1267 (1957).
[h] Can. J. Physics 37, 989 (1959).
[i] J. Sci. Ind. Res. 16B, 277 (1957).
[j] Proc. Roy. Soc. (London) A263, 494 (1961).

and comparable to the lattice heat capacity of our tin sample in the superconducting state.

The 340-g sample was a single crystal prepared for optical use (by the Harshaw Company). The crystal was activation-analyzed for Mn, Co, and Cu. The results of the analysis were: Cu, 0.27 ± 0.3 ppm; Mn, 0.0092 ± 0.0007 ppm; and Co, < 0.4 ppm.

Two separate runs were made on the KBr sample. Their results are listed in Table III. Figure 3 shows a plot of C/T vs T^2 for the KBr data. The line passing through the origin being the best fit to the higher temperature points, has a slope of 0.790 MJ $mole^{-1}$ deg^{-4}, giving a Debye theta of $\theta = 170.1^{\circ}K$. The lower-temperature points fall systematically above this line, being 1% high at $0.35^{\circ}K$, 5% high at $0.25^{\circ}K$ and 30% high at $0.12^{\circ}K$. This "excess" heat capacity can be represented by

$$C_{ex} = aT + b/T^2.$$

We believe that this excess heat capacity is an error in our addenda correction. This point is discussed in the next section.

Calculation of θ_0 from elastic constants by Alers and Neighbors[20] gives $\theta_0 = 172.8^{\circ}K$. This calculation is based on elastic constants extrapolated from $77^{\circ}K$. Betts, Bhatia, and Wyman,[21] using a different method of calculation, get $\theta_0 = 171.7^{\circ}K$. Heat-capacity measurements by Barron, Berg, and Morrison[22] yield a value of $\theta = 174^{\circ}K$; however, these measurements did not extend to temperatures low enough to get into the pure T^3 region.

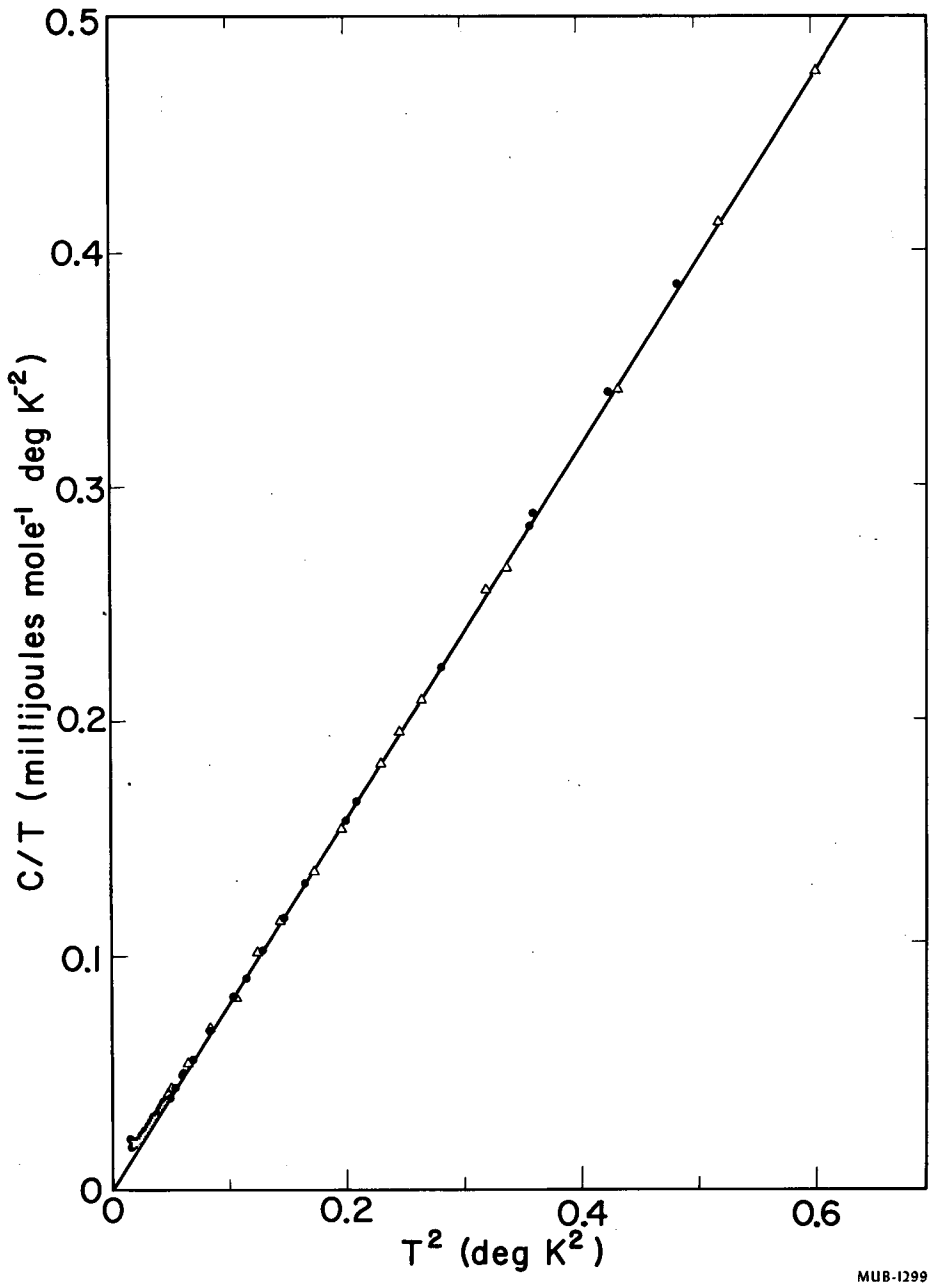

Fig. 3. The heat capacity of KBr. The symbols distinguish two separate runs.

Table III. Heat capacity of KBr.

First run			
T (^{o}K)	C (mJ/mole-deg)	T (^{o}K)	C (mJ/mole-deg)
.2534	.01323	.2898	.01990
.2787	.01788	.3520	.03562
.2502	.01388	.2188	.009038
.2189	.008800	.2428	.01205
.2199	.009155	.2675	.01559
.2205	.009580	.2973	.02152
.2628	.01535	.3291	.02911
.2887	.02036	.3492	.03381
.3120	.02493	.3802	.04374
.3209	.02836	.4159	.05649
.2248	.009581	.4157	.05695
.2542	.01392	.4427	.06789
.2786	.01768	.4796	.08109
.3013	.02223	.5303	.1175
.3101	.02482	.5814	.1541
.3373	.03128	.3963	.04952
.2397	.01156	.4322	.06394
.2690	.01601	.4520	.07263
.3005	.02225	.4962	.09684
.3241	.02751	.5145	.1074
.3400	.03192	.5663	.1449
.3589	.03716	.6033	.1737

Table III: (continued)

T (^{o}K)	C (mJ/mole-deg)	T (^{o}K)	C (mJ/mole-deg)
.3931	.04995	.6588	.2246
.4129	.05609	.7221	.3694
.3851	.04615	.8123	.4246
.4268	.06258	.8585	.5035
.2253	.009766	.8885	.5488
.2552	.01393	.9108	.5991
		Second run	
.1236	.002703	.2056	.007545
.1272	.002360	.2299	.01005
.1504	.003266	.2445	.01220
.1508	.003362	.2439	.01206
.1515	.003411	.2620	.01461
.1521	.003418	.2902	.01970
.1732	.004742	.3221	.02665
.1742	.004820	.3393	.03059
.1783	.005111	.3594	.03669
.1792	.005277	.3841	.04451
.1744	.004736	.4059	.05319
.1851	.005751	.4467	.07027
.1853	.005761	.4576	.07584
.1916	.006234	.5309	.1183
.1339	.002571	.5983	.1694
.1412	.002992	.6009	.1733
.1414	.002965	.6529	.2221
.1554	.003700	.6961	.2688
.1658	.004294	.7398	.3280
.1793	.005198	.8614	.5099
.1919	.006283		
.1906	.006195		
.2051	.007633		

Table III (continued)

T (^{o}K)	C (mJ/mole-deg)	T (^{o}K)	C (mJ/mole-deg)
.1852	.005451		
.1858	.005521		
.1953	.006495		
.2010	.006961		
.2015	.007111		
.2172	.008599		

D. Discussion of Errors

1. Errors associated with Temperature Determination

As stated in Sec. I, there are good reasons for believing that the temperature scale for cerium magnesium nitrate is correct. Here we assume it is, and go on to discuss some of the other errors in temperature determination.

Temperatures below $1^{\circ}K$ depend on the M(T) relationship as determined above $1^{\circ}K$. We can write this relationship as

$$M = M_0 + \frac{A}{T} ,$$

where M is the reading of the mutual inductance bridge, M_0 is the mutual inductance with the salt absent, and A is a constant proportional to the Curie constant for the salt. M_0 and A are determined from a plot of M vs 1/T.

To estimate errors in temperatures below $1^{\circ}K$ resulting from errors in determining the constant A and M_0, one can write

$$\frac{dT}{T} = \frac{dA}{A} + \frac{dM_0}{M - M_0} ,$$

where dT is the error in T resulting from errors of dA and dM_0 in A and M_0. And since in heat capacities it is the temperature differences that are important, we can write

$$\frac{dT_1}{T_1} = \frac{dA}{A} + \frac{dM}{M_1 - M_0} ,$$

and

$$\frac{dT_2}{T_2} = \frac{dA}{A} + \frac{dM}{M_2 - M_0} ;$$

and for the temperature difference ΔT we have

$$\Delta T + d\Delta T = T_2 + dT_2 - (T_1 + dT_1)$$

and

$$d\Delta T = T_2 \left(\frac{dA}{A} + \frac{dM_o}{M_2 - M_0}\right) - T_1 \left(\frac{dA}{A} + \frac{dM_0}{M_1 - M_0}\right).$$

We see then that the error in ΔT is of the same order of magnitude as the error in T. If T is in error, let us say by 1%, then ΔT and C will also be in error by 1%.

In examining our plots of M vs 1/T, and the probable accuracy of M and T measurements, we find an error of ±0.5% to be the largest that seems possible, and that an error of ±0.2% is more probable. We also note that near $1^{o}K$ any error in determining A from the plot tends to be partially compensated by an error in the opposite direction in M_0. In the low-temperature limit the error in M_0 becomes unimportant. We therefore conclude that errors of ±0.5% in A are possible, and that this would lead to errors in C/T of ±1% at the lowest temperatures.

Another possible source of error is lack of equilibrium between salt and sample when the resistance thermometer is being calibrated against the cerium magnesium nitrate. This had been a serious problem in the old apparatus, but did not seem to be as serious here. The effect shows up only at low temperatures ($0.1^{o}K$ or less), where equilibrium times tend to be long. and is such as to make the apparent T's too low by an amount that increases as T decreases. This makes the heat-capacity points appear low, since one thinks the ΔT's are larger than they actually are. It also shows up in the difference plot as a sharp kink in the curve at the lowest calibration points.

Error is also caused by not taking enough low-temperature calibration points to determine the difference plot unambiguously. If the difference plot is drawn incorrectly, it shows up as an artificial wiggle in the heat capacities. This difficulty can be avoided by taking many calibration points to temperatures well below the lowest temperature heat-capacity point. This was not possible in some of these experiments because (a) our 6000-Gauss magnet would take us down only to $0.08^{\circ}K$, and (b) during several of the experiments an excessive heat leak into the helium bath did not allow us the necessary time to take a large number of calibration points.

These last two sources of error could reasonably have caused the lowest-temperature points to be off by as much as several percent.

2. Errors Associated with Addenda Corrections at Low Temperature.

If the heat capacity of the "addenda" that is, anything in good thermal contact with the sample is either not small compared with that of the sample or is not accurately known, serious errors can be introduced into the measurements. The former leads to random errors and the latter to systematic errors. For normal metals only the second kind can be important, but for nonmetals or superconductors both can be important. This is because of the much larger heat capacity of normal metals at low temperatures.

For an experiment below $1^{\circ}K$ we had the following addenda: the copper thermal link going through the superconducting switch to the cooling salt and thermometer, the carbon resistance thermometer on the sample, the Manganin resistance heater, the G.E. 7031 varnish used to attach these addenda to the sample, the cotton threads used to mount the sample and

the Duco cement used to attach them, and the electrical leads to the heater and thermometer.

The thermal link and the support for the thermometer was of heavy copper wire, running between the sample and the superconducting switch. In ordinary commercial grade electrolytic copper, 99.99% pure with respect to other metals, dissolved oxygen may be present to the extent of 0.1%. Supposedly, the oxygen is present as copper oxide. The thermal link was weighed accurately and its heat capacity was assumed to be the same as that of the 99.999+ % materials that we had measured. This was almost certainly true within a few percent.

Contributions from the superconducting switch, and the indium used to solder it to the thermal link, were assumed to be negligible. Although it is possible to weigh the amount of indium used, one has no idea how much of the lead wire would be contributing. If one assumes that both are superconducting, neglecting their contribution is justified. However, it is possible that part of the combination is normal owing to frozen-in flux. Indeed, the presence of 0.5-g of normal indium would explain the high heat capacity of KBr at low temperatures.

The carbon resistance thermometer was a film of Aquadag (colloidal graphite) having a negligible heat capacity.

The resistance heater was made of Manganin, whose composition is 84% Cu, 12% Mn, and 4% Ni. Its heat capacity was measured (see Appendix) and goes as

$$C = \frac{0.0112}{T^2} + 0.0580\ T \text{ mJ/g-deg}$$

at low temperatures. Small and accurately measured amount of Manganin should not cause trouble except at the very lowest temperatures, where

it could dominate the heat capacity.

The heat capacity of G.E. 7031 varnish has been measured by Phillips,[18] and since only a small amount is used, it produces a small correction and cannot introduce serious errors.

The cotton threads and Duco cement were assumed negligible in effect. The leads to the heater and thermometer were of Manganin tinned with soft solder to make them superconducting. Superconducting leads are desirable because no power is dissipated in them. Since the leads were mostly Manganin, they had the large $1/T^2$ heat capacity; but unlike the heater, the leads were not in good thermal contact with the sample, so that not all of their heat capacity was being measured. Two separate experiments were carried out on KBr, differing only in the length of the leads. The change in heat capacity due to shortened leads was observable, but too small to account for the excess heat capacity in KBr. We found that if the leads are short, it is a good approximation to say that half their heat capacity contributes.

For small heat capacities, like that of KBr, addenda corrections can be quite important. In KBr it seems plausible that the excess heat capacity was caused by 0.5 g of normal indium in the switch. Addenda errors for normal metals will be much smaller, of the order of 1% at the most. For example, 1 g of normal indium would have only 0.2% of the heat capacity of our copper sample, at $0.1^{\circ}K$.

III. RESULTS

A. Indium

The measurements were made on a single crystal of cylindrical indium weighing 706 g (99.999+% pure, American Smelting and Refining Company, South Plainsfield, New Jersey). The heat-capacity data for both normal and superconducting states have been collected in Tables IV and V (A and B). These data, over the whole range of measurements, are plotted as C/T vs T^2 in Fig. 4.

The normal data below $2^{\circ}K$ can be represented by an equation of the form

$$C_N = C_q + \gamma T + \alpha T^3 + \beta T^5,$$

where C_q is the nuclear quadrupole heat capacity and is proportional to T^{-2}, as expected at temperatures high compared with the separation of the nuclear energy levels. The γT, and $\alpha T^3 + \beta T^5$, represent conventional separations into electronic and lattice heat capacities; C_q is determined by plotting CT^2 vs T^3 for the lowest temperature points. The intercept in this plot gives the T^{-2} coefficient and an approximate γ. The value determined for C_q is $1.01 \times 10^{-3}\ T^{-2}$ mJ/mole-deg. Then $C - C_q/T$ is plotted vs T^2. The slope gives an approximate α, and the intercept another approximate γ.

Figure 5 shows the data plotted in this way, together with the line given by $(C_N - C_q)/T = 1.69 + 1.42\ T^2$ vs T^2. Below about $0.3^{\circ}K$ the points systematically rise above the line, reaching a maximum of about 1% high at $0.12^{\circ}K$, after which the points drop sharply below the line, being as much as 5% low at $0.086^{\circ}K$. These effects are shown more clearly

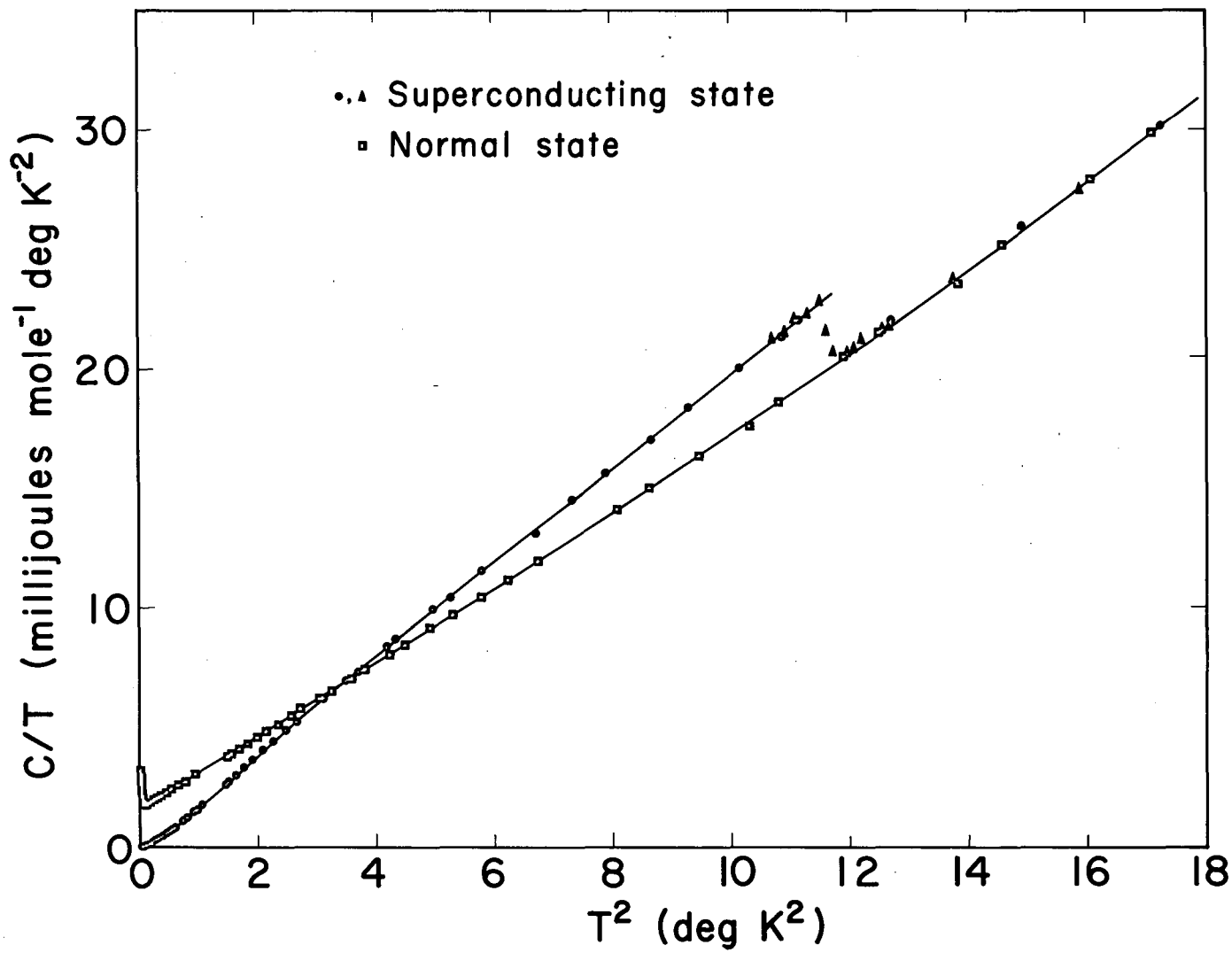

Fig. 4. The heat capacity of indium, 0.08 to 4.2 °K.

MUB-1281

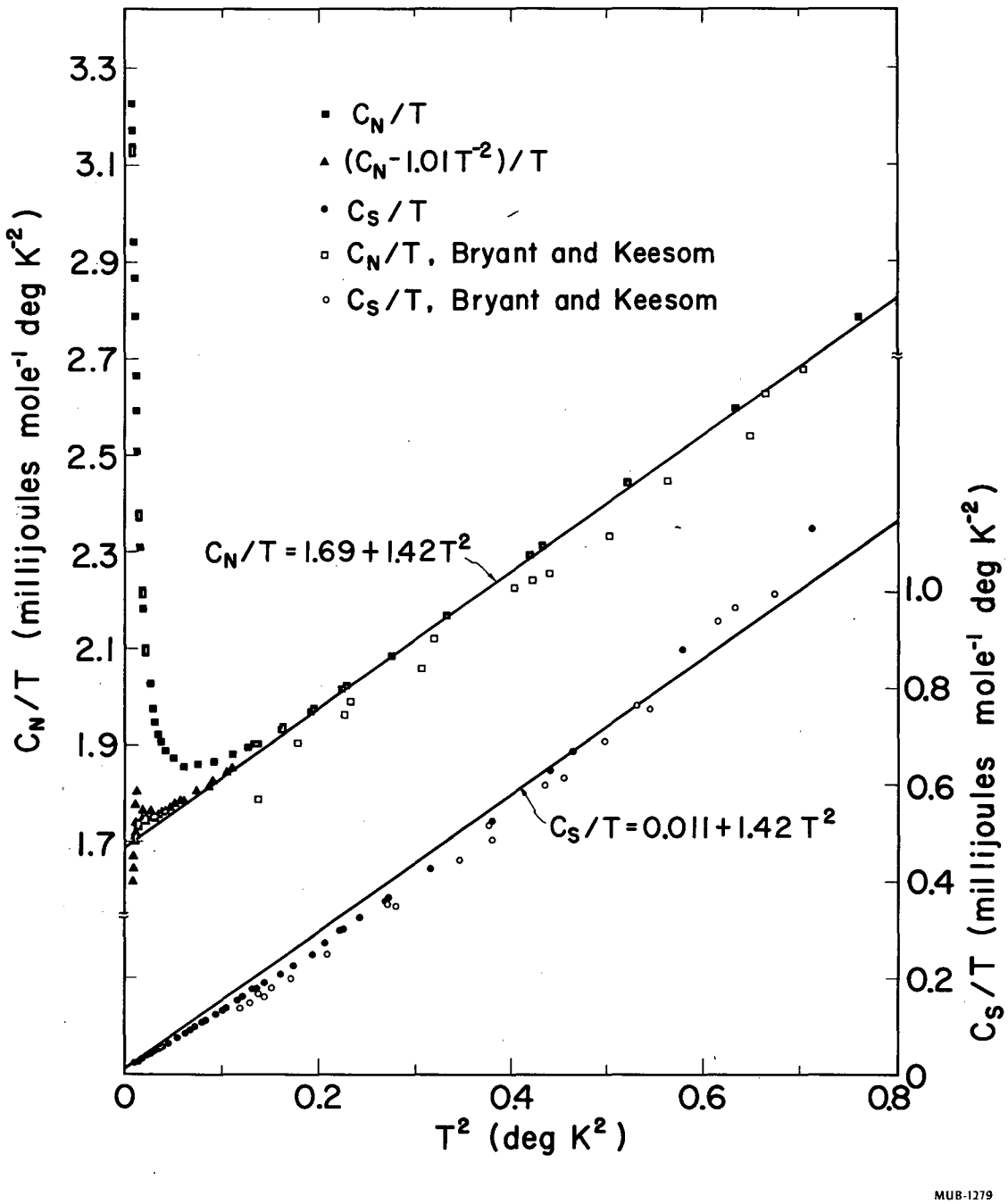

Fig. 5. The heat capacity of indium, 0.08 to 0.9 °K.

Table IV A. Heat capacity of indium below 1°K; H = 0 gauss.

(°K)	(mJ/mole-deg)	(°K)	(mJ/mole-deg)
.1051	.00258	.3178	.04286
.1064	.00310	.3494	.05667
.1131	.00298	.3686	.06528
.1149	.00334	.3796	.07241
.1168	.00366	.3229	.04558
.1175	.00343	.3245	.04562
.1329	.00452	.3402	.05271
.1407	.00504	.3635	.06396
.1412	.00508	.3792	.07187
.1422	.00527	.4006	.08360
.1515	.00590	.4175	.09425
.1524	.00596	.4388	.1094
.1603	.00674	.4543	.1234
.1608	.00666	.4766	.1440
.1639	.00717	.4932	.1605
.1643	.00709	.5191	.1852
.1679	.00756	.5223	.1905
.1689	.00782	.5091	.1735
.1841	.00933	.5604	.2338
.1928	.01065	.5633	.2407
.1965	.01129	.6183	.3240
.2113	.01368	.6647	.4182
.2130	.01424	.6821	.4565
.2329	.01788	.7618	.6708
.2385	.01901	.8450	.9553
.2506	.02174	.8915	1.155
.2581	.02374	.9750	1.560
.2610	.02431	.9501	1.453
.2708	.02729	1.0221	1.838
.2808	.02992		
.2834	.03082		
.2876	.03224		
.3066	.03860		

Table IV B. Heat capacity of indium below 1°K; H = 1000 gauss.

(°K)	(mJ/mole-deg)	(°K)	(mJ/mole-deg)
0.08560	0.2762	0.2210	0.4141
0.08659	0.2745	0.2362	0.4395
0.08774	0.2753	0.2439	0.4522
0.08897	0.2761	0.2630	0.4882
0.09231	0.2755	0.2703	0.5024
0.09532	0.2804	0.2908	0.5396
0.09575	0.2759	0.2990	0.5578
0.09884	0.2755	0.3003	0.5597
0.09995	0.2732	0.3207	0.6015
0.1055	0.2809	0.3298	0.6198
0.1055	0.2734	0.3304	0.6210
0.1095	0.2744	0.3535	0.6697
0.1166	0.2772	0.3620	0.6884
0.1170	0.2775	0.3652	0.6950
0.1214	0.2802	0.3997	0.7728
0.1288	0.2859	0.4011	0.7765
0.1296	0.2865	0.4357	0.8581
0.1344	0.2932	0.4396	0.8684
0.1422	0.2986	0.4726	0.9533
0.1425	0.2982	0.4773	0.9656
0.1570	0.3181	0.5239	1.092
0.1658	0.3273	0.5763	1.248
0.1705	0.3328	0.6466	1.455
0.1725	0.3357	0.6563	1.519
0.1824	0.3504	0.7955	2.073
0.1904	0.3627	0.7216	1.764
0.1906	0.3635	0.8721	2.427
0.2008	0.3794	0.9618	2.967
0.2118	0.3972		

Table V A. Heat capacity of indium above 1°K; H = 0 gauss

(°K)	(mJ/mole-deg)	(°K)	(mJ/mole-deg)
1.206	3.221	4.158	125.5
1.222	3.419		
1.274	3.863	(Using small Δ T's)	
1.326	5.591	3.345	73.80
1.381	5.084	3.409	73.52
1.444	5.905	3.475	72.46
1.503	6.669	3.544	76.61
1.572	7.751	3.271	69.28
1.630	8.594	3.303	70.82
1.767	11.03	3.331	73.42
1.866	13.09	3.393	77.31
1.919	14.11	3.361	74.88
2.044	17.21	3.425	70.84
2.092	18.23	3.458	7.145
2.230	22.27	3.493	74.05
2.297	24.07	3.527	77.22
2.407	27.89	3.562	77.67
2.506	31.12		
2.591	34.09		
2.715	39.48		
2.811	44.08		
2.945	50.28		
3.049	56.12		
3.191	64.11		
3.296	70.38		
3.565	78.57		
3.710	88.12		
3.862	100.3		
3.985	109.4		

Table V B. Heat capacity of indium above 1°K; H = 1000 gauss.

(°K)	(mJ/mole-deg)	(°K)	(mJ/mole-deg)
1.216	4.656	2.303	22.33
1.244	4.900	2.406	25.15
1.297	5.382	2.496	27.85
1.351	5.883	2.599	31.03
1.409	6.501	2.842	40.04
1.474	7.206	2.935	44.04
1.533	7.911	3.079	50.42
1.608	8.906	3.189	56.12
1.661	9.668	3.289	61.17
1.746	10.88	3.449	70.75
1.800	11.76	3.536	76.08
1.8940	13.40	3.720	87.62
1.952	14.50	3.818	96.11
2.056	16.54	4.009	111.0
2.120	17.91	4.145	123.9
2.225	20.41		

in Fig. 6, which shows only those points below $0.45^{\circ}K$. These deviations are comparable to those found for Cu and are assumed to be produced by systematic errors in the M(T) curve and the limiting slope of the difference plot. The α, β, and γ are finally determined from a plot of $(C-C_q-\gamma T)/T^3$ vs T^2 for various values of γ. The intercept in this plot is α and the slope is β. This plot is shown for four values of γ in Fig. 7. The value of 1.69 for γ was taken as the most reasonable choice, considering both the likelihood that the lowest points are high and also the very short region of validity of the $\alpha T^3 + \beta T^5$ approximation if the lowest points are given full weight. The values thus determined are

$$\alpha = 1.42 \text{ mJ/mole-deg}^4,$$

$$\beta = 0.0243 \text{ mJ/mole-deg}^6,$$

and

$$\gamma = 1.69 \text{ mJ/mole-deg}^2.$$

Bryant and Keesom, in their calorimetric work on two different samples,[23] have found $\alpha = 1.50$ and 1.53, $\gamma = 1.61$ and 1.59. Their points are shown with ours in Fig. 5. In the normal state, their lowest temperature points are about 3% below ours. At $1^{\circ}K$ the agreement is good; above $1^{\circ}K$ they are about 1% higher than ours.

The superconducting state below $1^{\circ}K$ is shown in Figs. 5 and 7. Below about $0.35^{\circ}K$, the superconducting state heat capacity is given by

$$0.0105\ T + 1.217\ T^3 \text{ mJ/mole-deg}.$$

The linear term is likely due to some normal indium trapped in the superconducting sample. The closeness of the indium sample to the demagnetization magnet (see Fig. 1) makes the sample normal when the

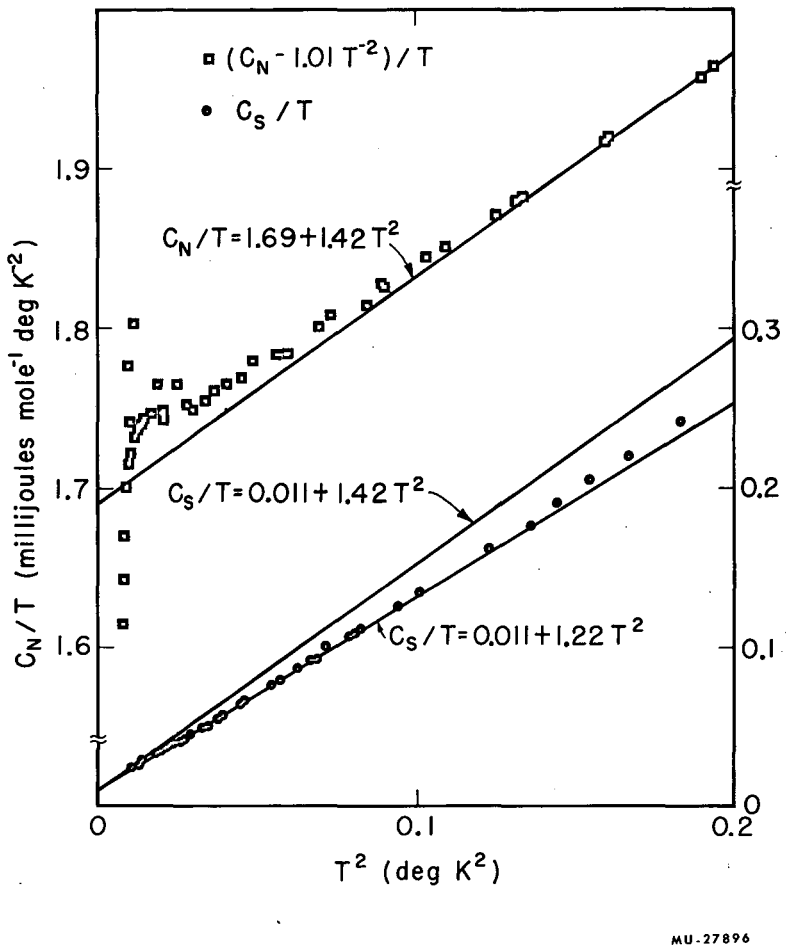

Fig. 6. The heat capacity of indium, 0.08 to 0.45 °K.

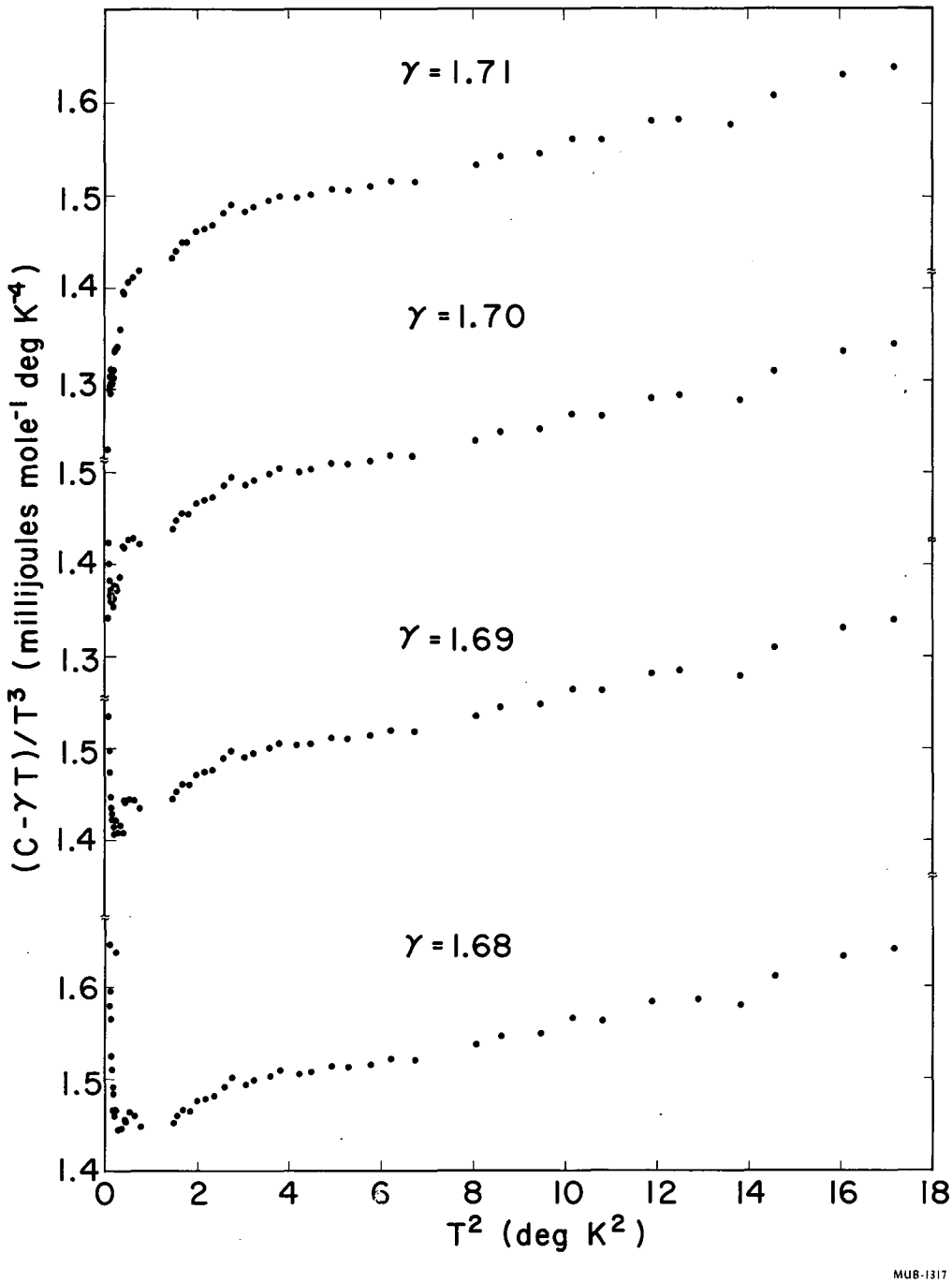

Fig. 7. The lattice heat capacity of normal indium.

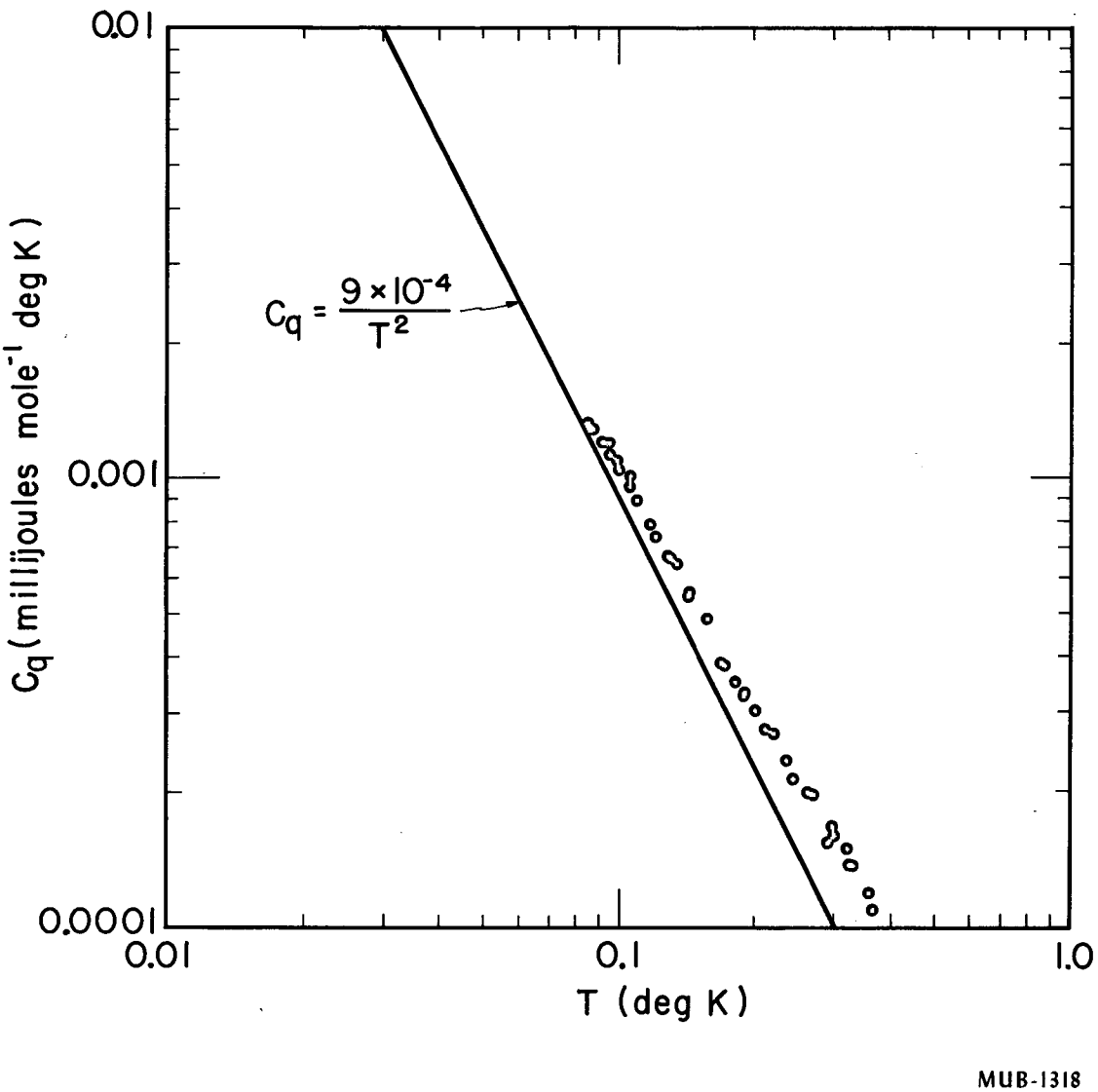

Fig. 8. The nuclear quadrupole heat capacity of indium.

copper potassium sulfate is magnetized. The magnetization curve is not reversible for nonellipsoidal shapes, or samples with mechanical flaws.[24] Thus when the magnetic field is turned off, about 0.6% of the sample remains in the normal state.

Two sets of measurements were carried out on the superconducting state, and they agreed well below about 0.4°K. Above this temperature the two sets of data progressively diverged until at 1°K they differed by 6%. This increased heat capacity in the second set of measurements was due to the influence of a magnetic field of several gauss on the sample. This field was too large to balance out with the earth's field-compensating coils. We subsequently learned that it resulted from frozen-in flux in the niobium coil around the sample.

The heat capacity of a superconductor in a magnetic field is greater than that of a mixture of superconducting and normal material by an amount $Q(dX/dt)$, where Q is the latent heat and dX the amount transformed. One can write[27]

$$C = XC_N + (1-X)C_S + Q\frac{dX}{dT},$$

where X = amount of normal material, and $Q = -VT(H_c/4\pi)(dH_c/dt)$. Using this equation, and a parabolic critical field, one can estimate how much material would need to transform at a given temperature to make a heat-capacity point a given amount high. Doing this, one finds that 6%/deg is required at 1°K to make a heat-capacity point 6% high. This seems not unreasonable. The other set of measurements was made with the niobium coil absent and fitted smoothly onto the above 1°K measurements.

As in the normal state, our superconducting points are higher than

those of Bryant and Keesom at low temperatures.[22] At their lowest temperatures their points are about 8% below ours; this is with the linear term subtracted from our points. At 1°K and above, agreement is good. The heat-capacity points of Bryant and Keesom are also shown in Fig. 5.

The critical magnetic field at which the normal and superconducting phases are in equilibrium can be calculated from the heat capacity by the thermodynamic expression

$$H_C^{\,2}(T) = \int_{T_C}^{T} dT \int_{0}^{T_C} \frac{C_S - C_N}{T}\, dT.$$

The transition temperature T_C was chosen to be the temperature at which the entropy difference vanished; that is, $T_c = 3.405°K$. The critical field at 0°K was calculated to be 285 gauss. This compared to the value of 282.66 gauss obtained by Finnemore and Mapother from direct critical field measurements at low temperatures.[28] Bryant and Keesom calculated a value of 284 gauss from their heat-capacity work.

A more sensitive comparison with the critical-field data is made by plotting the deviation function D(t) vs t^2:

$$D(t) = h - (1 - t^2),$$

where $t = T/T_C$, and $h = H/H_C$. In our calculation of D(t), shown in Fig. 9 together with the measurements by Finnemore and Mapother, the agreement is excellent. Figure 10 shows the low-temperature section D(t) in more detail.

If one assumes the superconducting electronic heat capacity to be given by

$$C_{ES} = C_S - 1.217\, T^3 - 0.0105 \text{ mJ/mole-deg},$$

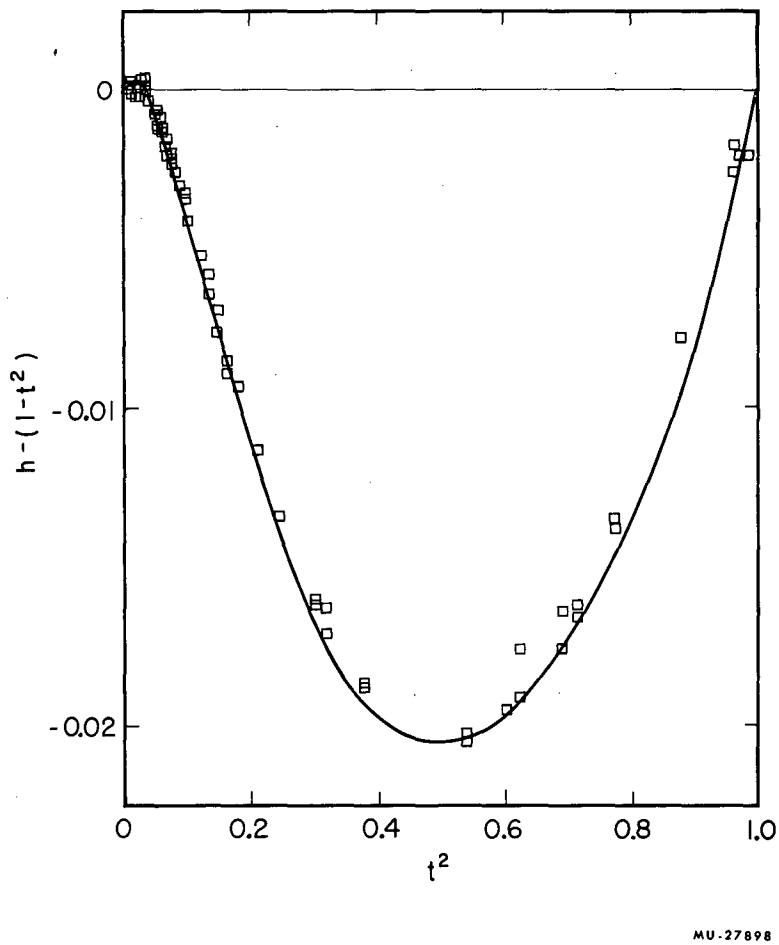

Fig. 9. The deviation of the critical field of indium from a parabola.

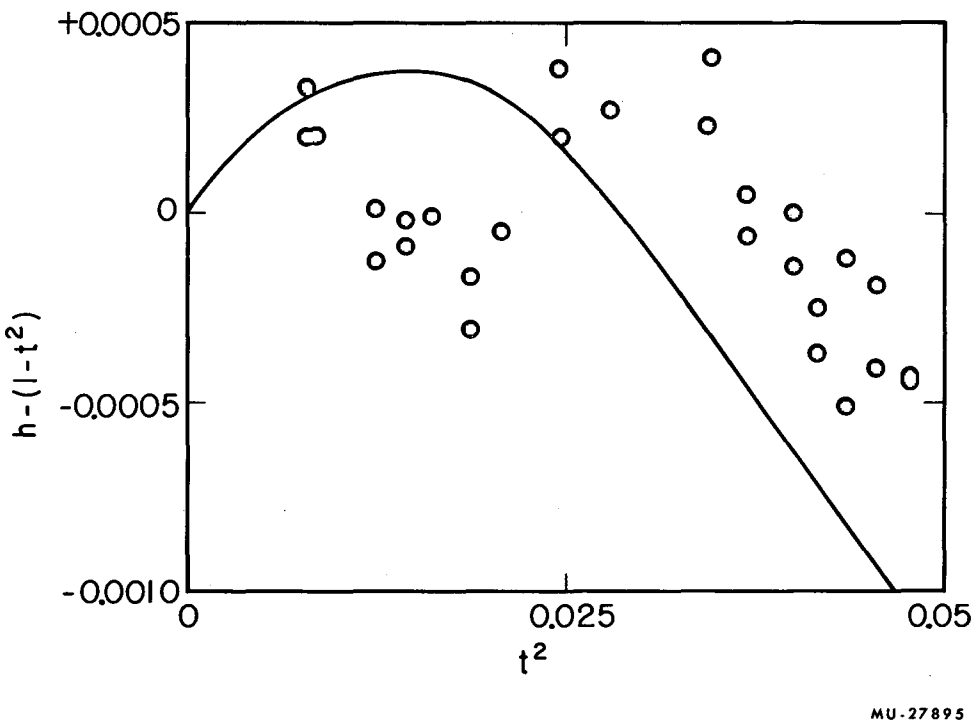

Fig. 10. The deviation of the critical field of indium from a parabola, at the lowest temperature.

and fits the data to an exponential in temperature, one finds

$$\frac{C_{ES}}{\gamma T_C} = 8.25 \exp\left[-1.34\ T_C\right]/T$$

A semilog plot of $C_{ES}/\gamma T_C$ vs T_C/T is shown in Fig. 11.

B. Tin

Tin of 99.9999% purity was purchased (Cominco Products, Inc., Spokane, Washington). The measurements were made on a polycrystalline sample of cylindrical shape weighing 843 grams. The heat-capacity data for both normal and superconducting states have been collected in Table VI (A-B).

The tin experiment differs from the previous experiments described, in that the indium used to solder the thermal link from the sample to the lead wire of the superconducting switch was eliminated. The thermal link was instead connected to the lead wire by G.E. 7031 varnish. This removed the possibility that normal indium, with its large heat capacity, would interfere with the superconducting tin measurements. The data are shown plotted as C/T vs T^2 in Figs. 12 and 13. Figure 12 extends over the complete range of measurements; Fig. 13 includes only points below $0.45^{\circ}K$. Below about $0.45^{\circ}K$ the superconducting-state heat capacity is given by

$$0.004\ T + 0.246\ T^3\ \text{mJ/mole-deg.}$$

Tin, like indium, shows a linear term in the superconducting state. This again is attributable to a small amount of normal material present during the superconducting-state measurements; C_{LS} is then $0.246\ T^3$ mJ/mole-deg.

Bryant and Keesom's data[22] are also shown in Fig. 12. Their

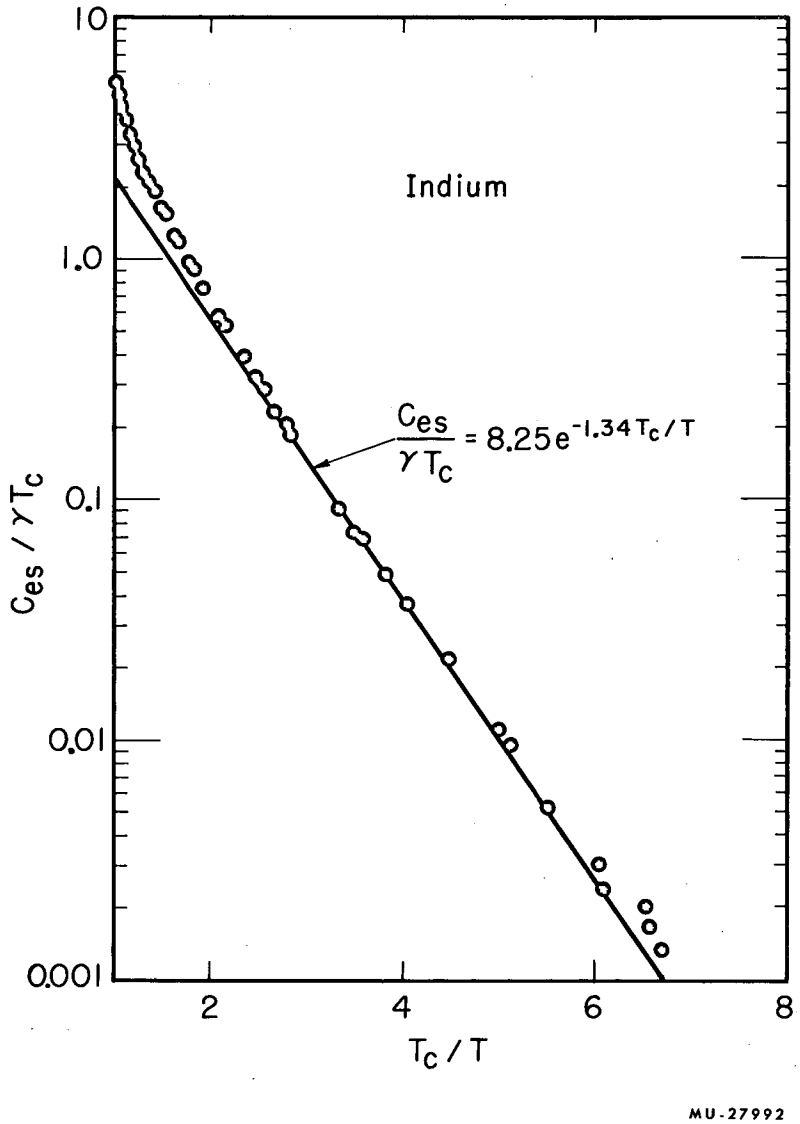

Fig. 11. The superconducting electronic heat capacity of indium.

Table VI A. Heat capacity of tin below 1°K; H = 0 gauss.

(°K)	(mJ/mole-deg)	(°K)	(mJ/mole-deg)	(°K)	(mJ/mole-deg)
0.1456	0.001585	0.3537	0.01218	0.3543	0.01231
0.1519	0.001461	0.3635	0.01332	0.3636	0.01329
0.1569	0.001566	0.3577	0.01282	0.3736	0.01433
0.1667	0.001870	0.3672	0.01359	0.3881	0.01590
0.1676	0.001902	0.3703	0.01392	0.3900	0.01620
0.1720	0.001921	0.1558	0.001647	0.4058	0.01807
0.2305	0.003998	0.1601	0.001673	0.4112	0.01892
0.2380	0.004477	0.1616	0.001800	0.4276	0.02208
0.2384	0.004429	0.1725	0.002074	0.4419	0.02327
0.2523	0.004629	0.1770	0.002139	0.4434	0.02339
0.2539	0.004953	0.2009	0.002925	0.4554	0.02552
0.2540	0.005036	0.2014	0.002892	0.4837	0.03032
0.2572	0.005063	0.2174	0.003514	0.5150	0.03698
0.2575	0.005052	0.2279	0.003913	0.5383	0.04298
0.2818	0.006604	0.2288	0.004013	0.5749	0.05460
0.2875	0.006939	0.2333	0.004129	0.5826	0.05661
0.2884	0.007198	0.2338	0.004060	0.6170	0.07003
0.2894	0.007019	0.2340	0.004179	0.6557	0.07992
0.2914	0.007282	0.2345	0.004058	0.7016	0.1150
0.2981	0.007626	0.2525	0.004968	0.7879	0.1887
0.3024	0.007996	0.2564	0.005300	0.8596	0.2714
0.3067	0.008135	0.2667	0.005724	0.9203	0.3642
0.3128	0.008928	0.2831	0.006727	0.9564	0.4271
0.3178	0.009192	0.2840	0.006765	1.061	0.6489
0.3195	0.009500	0.3021	0.008097	1.243	1.195
0.3200	0.009459	0.3082	0.008556		
0.3333	0.01029	0.3242	0.009727		
0.3382	0.01056	0.3287	0.01009		
0.3402	0.01118	0.3367	0.01075		

Table VI B. Heat capacity of tin below 1°K; H = 1000 gauss.

(°K)	(mJ/mole-deg)	(°K)	(mJ/mole-deg)	(°K)	(mJ/mole-deg)
0.09269	0.1615	0.1780	0.3141	0.3973	0.7153
0.09474	0.1645	0.1821	0.3204	0.4339	0.7928
0.09517	0.1658	0.1865	0.3297	0.4408	0.7998
0.10373	0.1754	0.1966	0.3493	0.4886	0.8998
0.10470	0.1756	0.2003	0.3529	0.5137	0.9439
0.11136	0.1887	0.2051	0.3646	0.5264	0.9734
0.11165	0.1887	0.2182	0.3888	0.5423	1.003
0.11734	0.2043	0.2204	0.3913	0.5681	1.057
0.11868	0.2085	0.2301	0.4088	0.6260	1.180
0.1217	0.2162	0.2402	0.4266	0.6374	1.204
0.1286	0.2318	0.2438	0.4313	0.6923	1.319
0.1315	0.2369	0.2594	0.4616	0.6932	1.325
0.1342	0.2367	0.2652	0.4737	0.7637	1.473
0.1410	0.2488	0.2888	0.5148	0.8199	1.597
0.1453	0.2555	0.2925	0.5209	0.8393	1.643
0.1480	0.2597	0.2978	0.5301	0.8941	1.774
0.1485	0.2602	0.3198	0.5727	0.9341	1.862
0.1603	0.2797	0.3592	0.6647	0.9637	1.944
0.1625	0.2847	0.3550	0.6362	1.032	2.107
0.1652	0.2900	0.3948	0.7158	1.037	2.110
				1.126	2.338

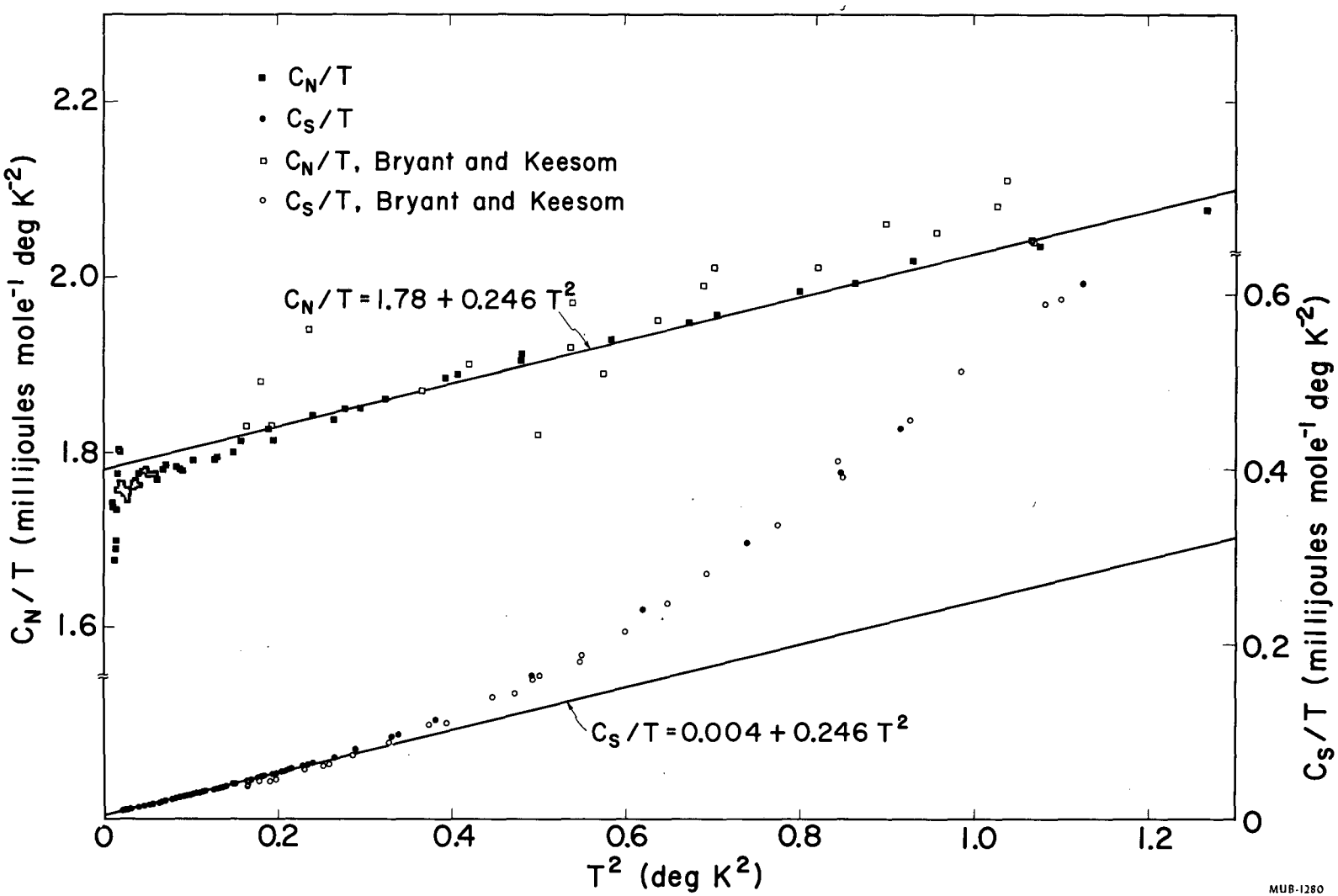

Fig. 12. The heat capacity of tin.

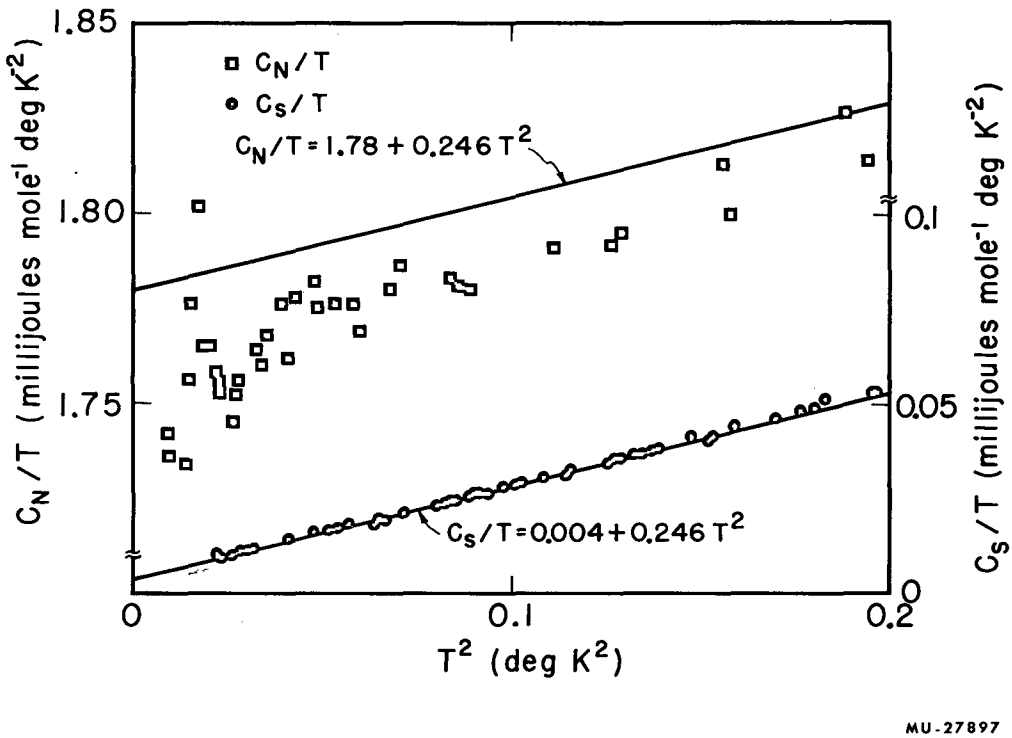

Fig. 13. The heat capacity of tin below 0.45 °K.

points are about 3% below ours at their lowest temperatures, with the linear term subtracted from our data. At $1^{\circ}K$ our agreement is good.

The superconducting electronic term C_{ES} is taken to be $C_S - 0.246\ T^3$. Figure 14 shows a semilog plot of $C_{ES}/\gamma T_c$ vs T_c/T. This gives us $C_{ES}/\gamma T_c = 7.85 \exp\left[-1.42\ T_C\right]/T$.

In the normal state the lattice heat capacity is only 12% of the total, even at $1^{\circ}K$, making an accurate evaluation of C_{LN} difficult. A line given by $C_{N/T} = 1.78 + 0.246\ T^2$, which has the same slope as $C_{S/T}$ in the low-temperature limit, is an adequate representation of the data. It is noted that for tin, unlike copper and indium, the lowest temperature points fall below the line that is the best fit to the higher temperature points.

The data of Bryant and Keesom[22] are compared with ours in Fig. 12. Their points are from 2 to 3% higher than ours, even at $1^{\circ}K$. Their normal-state indium points are about the same amount lower than ours. By least-squares analysis, Bryant and Keesom get $\gamma = 180$ and $\alpha = 0.242$.[1] Corak and Satterthwaite, in their calorimetric work above $1^{\circ}K$, have found $\gamma = 1.75$ and $\alpha = 0.262$.[29]

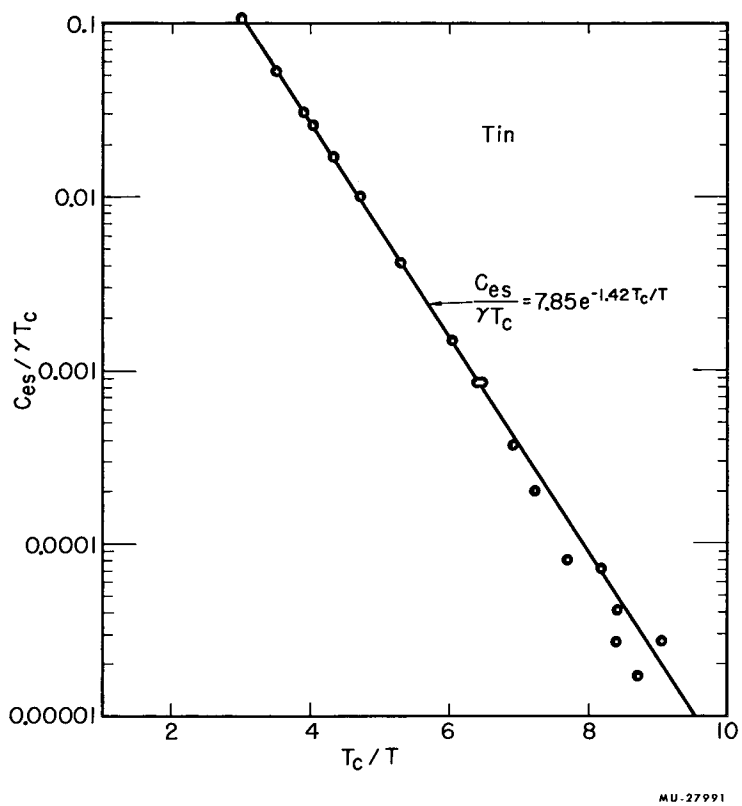

Fig. 14. The superconductive electronic heat capacity of tin.

IV. DISCUSSION

Comparison of our work on tin and indium with other pertinent experiments is summarized in Table VII.

A. Nuclear Quadrupole Heat Capacity

Figure 8 shows C_q for indium derived as $C_q = C_N - 1.69\ T - 1.42\ T^3 - 0.024\ T^5$, plotted vs T on a log-log scale. The line was calculated from the nuclear resonance data.[31,32] The difference between the resonance value and ours is 10%. This discrepancy is not surprising, considering that C_q is a significant fraction of the total heat capacity over only a very short temperature interval. Furthermore, these are the lowest temperature points, in which the experimental uncertainty is greatest. Above about 0.12°K our points appear to deviate from a T^{-2} temperature dependence. However, this is merely the systematic deviation between 0.12°K and 0.30°K mentioned above.

It is also possible that the discrepancy between C_q and resonance data is a consequence of defects. Defects might be expected to increase the field gradients in their neighborhood. This effect would probably not show up in nuclear quadrupole resonance experiements; only the contribution from unstrained regions would be observed, or the line would be broadened to the extent that the resonance is not observed.

In the superconducting state no T^{-2} contribution to the heat capacity appears. We interpret this as showing that the nuclear spin-lattice relaxation time T_1 is long compared with the 2 or 3 minutes required to make a heat-capacity measurement. An estimated T_1 of 8 seconds for normal indium at 0.1°K is obtained by applying the

Table VII. Comparisons with related measurements

Tin	γ	α_N	α_S	T_C	H_0	$10^3 \times C_q T^2$
This work	1.78	0.246	0.246			
Bryant & Keesom[a] (calorimetric)	1.80	0.242	0.242	3.701	306	
Corak & Satterthwaite[b] (calorimetric)	1.75	0.262	0.262	3.722	303.4	
Rayne & Chandrasekhar[c] (elastic constants)		0.238	0.238			
Finnemore & Mapother[d] (critical field)	1.74			3.722	305.50	

Indium	γ	α_N	α_S	T_C	H_0	$10^3 \times C_q T^2$
This work	1.69	1.42	1.22	3.405	285	1.01
Bryant & Keesom[a] (calorimetric) (I)	1.61	1.50	≈1.1	3.403	284	
(II)	1.59	1.53				
Chandrasekhar & Rayne[c] (elastic constants)		1.41	1.41			
Finnemore & Mapother[d] (critical field)	1.66			3.407	282.66	
Simmons & Slichter[f]						
Hewitt & Knight[g] (nuclear resonance)						0.901

[a]See reference 23.

[b]See reference 29.

[c]See reference 30.

[d]See reference 28.

[e]See reference 4.

[f]See reference 31.

[g]See reference 32.

Korringa relation to Knight-shift data for liquid indium. The equality of the shift in solid and liquid has been discussed by Knight and Berger.[25] We could not detect relaxation effects in the normal-state measurements and concluded therefore that $T_1 < 5$ sec. The estimated increase in T_1 for the superconducting state[26] could explain our observations.

B. Lattice Heat Capacity

The most striking feature of the results is that for superconducting indium below $0.7^{\circ}K$, the total heat capacity is less than the calculated contribution for sound waves alone. On the other hand, the conventional analysis of the normal-state data gave the expected value for the lattice heat capacity. For tin no such discrepancy was observed.

In principle, the discrepancy between normal- and superconducting-state lattice heat capacities should show up in critical field measurements. Finnemore and Mapother have measured the critical field for indium down to $0.3^{\circ}K$.[28] A comparison of our data with theirs is given in Figs. 9 and 10 as $D(t)$ vs t^2, where $D(t) = h - (1 - t^2)$. The agreement in general is excellent. The positive initial slope in our $D(t)$ curve is a necessary consequence of the T^3 term in our $C_N - C_S$. The critical-field measurements lack the precision necessary to show the existence of this feature. This reflects the insensitivity of critical-field measurements to the thermodynamic properties of the superconducting state at low temperatures.

If, as seems likely, the linear term in the superconducting-state heat capacity is associated with the presence of frozen-in flux, C_S

is proportional to T^3 at the lowest temperatures. Assuming that C_S is the sum of separable lattice and electronic terms, and further that the electronic term goes to zero more rapidly than T^3, we have found C_{LS} of indium proportional to T^3 above 0.1^oK, and up to at least 0.4^oK. On the basis of the usual relation between phonon-spectrum and lattice heat capacity, this shows that there is no dispersion for lattice vibrations at frequencies corresponding to this temperature range. C_{LN} is also proportional to T^3 but is 16% greater than C_{LS}, showing that the sound velocities are different in the two states for the thermally excited modes (approximately 2000 Mc/sec to 8000 Mc/sec, corresponding to 0.1^oK to 0.4^oK). The measurements by Chandrasekhar and Rayne[4] show that at 10 Mc/sec the sound velocities are in excellent agreement with the observed C_{LN}, and are the same in the two states to within 2×10^{-2}%. It follows that there must be a dispersion in the superconducting state between 10 and 2000 Mc/sec. Dransfeld has failed to detect a difference in sound velocities between the normal and superconducting states at 1000 Mc/sec.[38]

Ferrell has suggested a dispersion mechanism for wave lengths greater than the coherence distance but energies less than the gap energy.[33] For indium, this corresponds to the frequency range 1.3×10^3 to 2×10^5 Mc/sec, or temperatures between 0.065 and 10^oK. Ferrell derived

$$C_{LS} = \alpha T^3 - BT^2,$$

where α is the normal-state T^3 coefficient, and the T^2 term is first-order in the anomaly. The T^2 coefficient is related to α as

$$B = 0.556 \frac{\hbar\Delta\omega}{k} \alpha.$$

Term $\Delta\omega$ is the magnitude of the frequency shift, and is the same for all affected modes. The $\hbar$ is Planck's constant and k is Boltzmann's constant. By plotting C_S/T^2 vs T, one should get a straight line with a negative intercept, this negative intercept being B. This plot is shown in Fig. 15, the superconducting points having had the linear term subtracted. Using $\alpha = 1.42$, we get $B = +0.08$. Ferrell argues that below $0.065^{\circ}K$ the dispersion will not be important and C_S will go into αT^3. Our points start deviating, not at $0.065^{\circ}K$, but at $0.4^{\circ}K$ and, in fact, do not show the existence of a T^2 term at all. The T^2 terms in Ferrell's expression for C_{LS} are a consequence of the constant shift $\Delta\omega$ for thermally excited modes. The heat-capacity data require a frequency shift proportional to frequency, as so to give constant sound velocities.

Daunt and Olsen have suggested that the behavior of indium might be explained by a difference in the temperature dependence of the zero-point energy between the two states.[34] One can write, for the energy of a Debye solid,

$$E = \frac{9}{8} R\Theta + A \frac{T^4}{\Theta^3} ,$$

and if Θ is temperature-dependent,

$$C = \frac{9}{8} R \frac{\partial\Theta}{\partial T} + 4A \frac{T^3}{\Theta^3} - 3A \frac{T^4}{\Theta^4} \frac{\partial\Theta}{\partial T} .$$

If $\frac{\partial\Theta}{\partial T} \approx -10^{-6}$ it would be of the right order of magnitude to explain the heat-capacity measurements. Daunt and Olsen's argument assumes the Debye model, but would apply qualitatively to more realistic frequency spectra if the assumption that the temperature dependence of all frequencies can be derived from the temperature dependence of

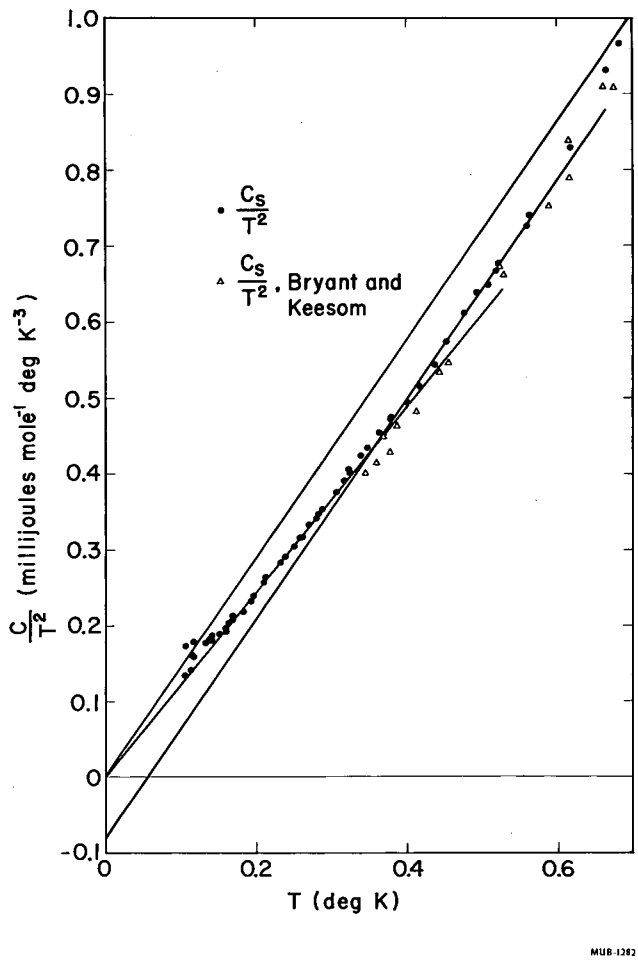

Fig. 15. The superconductive state heat capacity of indium, plotted to test Ferrell's dispersion relation.

θ_0 is correct. This is probably not a good assumption, however, and leads to the conclusion that for all solids with temperature-dependent elastic moduli there should be a contribution of this type to the heat capacity. The absence of this contribution is shown by the generally good agreement between measured lattice heat capacities and that calculated from elastic constants. Also, to assume that the lattice internal energy can be written separately, disregarding the electrons, is to ignore the interaction that gives rise to superconductivity, and it is probably these electron-lattice terms which are most important. Since the contribution of Daunt and Olsen gives rise to a latent heat at T_C, it is implied that there must be other terms that compensate for this entropy difference and bring it to zero at T_C. In following their calculation through, Daunt and Olsen found a contribution to the heat capacity of $\Delta C_L = AT + BT^3$. However, this is probably due only to their assumption of a parabolic critical field. It is not clear whether changes in zero-point energy need to be taken into account explicitly, or whether they have been taken into account automatically. For example, Ferrell suggests that these changes are already included and appear as a "renormalization of the single-electron excitation energies." However, Ferrell's argument that thermodynamic laws preclude a contribution from zero-point effects " ... according to the second law of thermodynamics, a physical system can only take on heat by means of an increase in its entropy, or disorder. If the high-frequency lattice oscillators remain in their ground states, their quantum numbers do not change and they cannot directly contribute any disorder to the system..."

is not valid. The second law of thermodynamics requires only that there be an increase in entropy for the whole collection of normal modes, not just the high-frequency ones. Although the basic idea of Daunt and Olsen may possibly be correct, certainly their method of calculating its magnitude is incorrect.

As mentioned earlier, Chester,[11] and Marcus and Maxwell,[12] have both shown that if the similarity principle is obeyed there should be no difference in the lattice heat capacity between the two states. Senozan and Phillips have recently measured the critical-field curves for In^{113} and In^{115} and have found H_0 and T_c proportional to $M^{-0.56}$.[35] Within the experimental scatter, the similarity principle holds for indium. It is of interest, then, to estimate the magnitude of the deviations from the similarity principle owing to the differences in lattice heat capacity that we observe in indium. An estimate can be made using the two-fluid model of Marcus and Maxwell.[11] They have derived for the reduced critical field the expression

$$h^2 = \omega_e + t^2 \frac{[1 - K(\omega_e)]}{K'(0)} - t^2 \frac{[1 - K(\omega_e)]}{\beta K(0)} \frac{\partial F_L(T,\omega_e)}{\partial \omega_e} + \frac{1}{\beta}[F(T,0) - F_L(T,\omega_e)], \qquad (1)$$

where $h = H/H_0$ and $t = T/T_c$, and where ω is the parameter measuring the degree of condensation into the superconducting state, ω_e is the equilibrium value of ω at a given temperature, $\omega_e = 0$ at $T = T_c$, and $\omega_e = 1$ at $T = 0$. $K(\omega)$ is the effective number of electrons, $F_L(T,0)$ and $F_L(T,\omega_e)$ are the lattice free energies of the normal and superconducting states respectively, and β is the difference in

free energy at $0^{\circ}K$, $H_0^2 V_M/8\Pi$. The last two terms in Eq. (1) arise only if the lattice free energies are difference in the two states.

For purpose of making this estimate, we assume a parabolic critical field, for which

$$K(\omega_e) = (1 - \omega_e)^{1/2}$$

and

$$\omega_e = (1 - t^4).$$

Equation (1) then simplifies to

$$h^2 = (1 - t^2) - \frac{t^2}{\beta}(1 - t^2)\frac{\partial F_L}{\partial \omega_e}(T,\omega_e) + \frac{1}{\beta}[F_L(T,0) - F_L(T,\omega_e)].$$

Since only the last two terms are dependent on isotopic mass, we write them as

$$\Delta = -\frac{t^2}{\beta}(1 - t^2)\frac{\partial F_L}{\partial \omega_e}(T,\omega_e) + \frac{1}{\beta}[F_L(T,0) - F_L(T,\omega_e)]. \qquad (2)$$

If we assume a T^3 heat capacity, F_L depends on mass as $M^{3/2}$, and since H_0 depends on mass approximately as $M^{-1/2}$, β depends on mass as M^{-1}. The Δ then will vary with mass as $M^{5/2}$.

To calculate Δ we need to know the temperature dependence of $F_L(T,\omega_e)$. Our heat-capacity results tell us that at sufficiently low temperatures $C_{LS} < C_{LN}$. One possible assumption is that the lattice heat capacity changes discontinuously at T_C in such a way that below T_C, $C_{LN} = 1.42\ T^3$, and $C_{LS} = 1.22\ T^3$. In this case, F_L will be independent of ω and only the second term in Δ will contribute, or

$$\Delta = \frac{1}{\beta}(-167\ T^4);$$

and since

$$\beta = 4.89 \times 10^4 \text{ ergs/mole},$$

$$\Delta = -0.652 \text{ at } T = T_C,$$

which must be compensated by other terms in the free energy so that $\Delta F = 0$ at $T = T_C$. But this large mass-dependent contribution to the free energy would produce an easily detectable deviation from the similarity principle, which has not been observed.

Another possible assumption is that the difference in lattice free energy is proportional to ω_e, i.e.,

$$F_L(T,\omega_e) = F_L(T,0) - 0.15\, F_L(T,0)\omega_e .$$

The 0.15 in the fractional amount C_{LS} is less than C_{LN} at low temperatures. Calculating Δ from this free-energy relationship, one gets

$T(^{\circ}K)$	Δ
$T_C = 3.405$	0
3	-.1676
2	-.0641
1	-.0039
0	0

Although the values of Δ are smaller, and their temperature dependence different in this case, one should still be able to detect deviations from the similarity principle.

Indeed, the only kind of change in lattice heat capacity of the observed size that would not produce measurable deviations from the similarity principle would be one that did not extend above $0.8^{\circ}K$. Such a change would not produce deviations from the similarity principle because its contribution would be a small part of the total free-energy difference.

Finally, we wish to draw attention to the fact that our measurements by themselves do not completely exclude a value of α of approximately

1.22 for both states. This value could be obtained for the normal state if only data below $0.25^{\circ}K$ were used to estimate the limiting slope of C/T vs T^2. Such an interpretation gives more weight to the lowest temperature points than we believe justified, and the measured γ would differ from that calculated from critical fields by more than we expect. Furthermore, although this interpretation eliminates the anomalous difference between α_N and α_S, it still leaves us with two anomalous features. The lattice heat capacity is less than that calculated from sound velocities for both states, and it has a temperature dependence without parallel, C_L being approximated by $\alpha T^3 + \beta T^5$ only up to $0.5^{\circ}K$, or $\Theta_0/200$ (see fig. 6). On the whole, we consider this interpretation less likely.

C. Electronic Heat Capacity

The BCS[3] theory gives for the superconducting electronic heat capacity, in this temperature range, $C_{ES}/\gamma T_C = 8.5 \exp [-1.44\ T_C]/T$, and for the energy gap at $0^{\circ}K$, $3.50\ kT_C$. One can estimate the energy gap from our heat-capacity data as, for tin:

$$\frac{1.42}{1.44} \times 3.50\ kT_C = 3.45\ kT_C,$$

and for indium:

$$\frac{1.34}{1.44} \times 3.50\ kT_C = 3.26\ kT_C.$$

Other determinations of the energy gap for tin and indium are shown in Table VIII.

Our value of $3.26\ kT_C$ for the energy gap of indium is appreciably lower than the other values given in the table. This may be because we have assumed that C_{LS}/T^3 remains constant and equal to the low-temperature limiting value.

Table VIII. Energy gap in tin and indium

	Tin	Indium
This work	3.45	3.26
Critical field[a]	3.60	3.64
Infrared absorption in bulk samples[b]	3.6 ± 0.2	4.1 ± 0.2
Infrared absorption in their films[c]	3.3 ± 0.2	3.9 ± 0.3
Election tunneling[d]	3.46 ± 0.10	3.64 ± 0.10

a. See reference 27

b. Richards and Tinkham, Phys. Rev. 119, 575 (1960).

c. Ginsberg and Tinkham, Phys. Rev. 118, 990 (1960).

d. Giawer and Megerle, Phys. Rev. 112, 1101 (1961).

APPENDIX

Heat Capacity of Manganin

The heat capacity of manganin was measured from 0.25°K to 4.2°K. Manganin has an approximate composition of 84% Cu, 12% Mn, and 4% Ni. The measurements were made on a 1000-g sample (Driver-Harris Company, Harrison, New Jersey). A plot of C vs T is shown in Fig. 16. The low-temperature heat capacity can be represented as

$$C = 0.0580\ T + \frac{0.0112}{T^2}\ \text{mJ/g-deg.}$$

This relationship holds below about 1.5°K.

The T^{-2} contribution is attributed to the ordering of the nuclear spin of the manganese ions by the electron spins. The nuclear spin in $I = 5/2$, and the spin of the manganese ion is supposedly $S = 5/2$. Similar results have been obtained by du Chatenier and de Nobel on dilute alloys of manganese in copper.[34] These experiments, together with the above described experiments at 1°K by Zimmerman and Sato on concentrated manganese-copper alloys,[37] suggests that the T^{-2} coefficient is at least roughly proportional to the Mn concentration. This is an interesting result and experiments below 1°K on the concentrated alloys should be done to check this point.

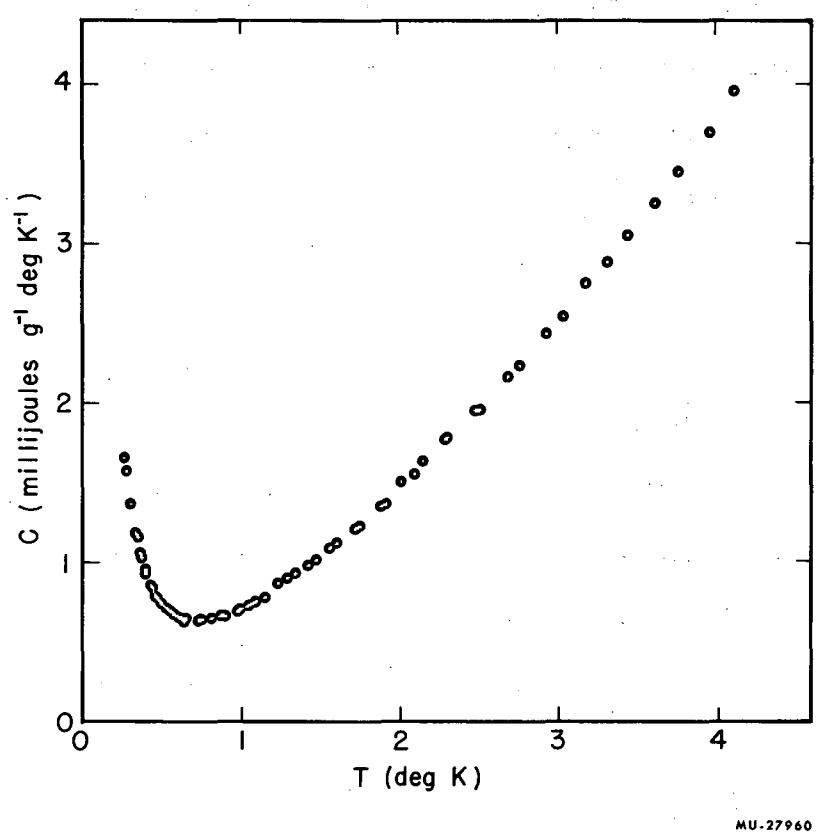

Fig. 16. The heat capacity of manganin.

ACKNOWLEDGMENTS

The author wises to express his sincere appreciation for the inspiring guidance of Professor Norman C. Phillips, whose advice, encouragement, and unbounded interest provided a large contribution toward the completion of this work.

This work was performed under the auspices of the U.S. Atomic Energy Commission.

REFERENCES

1. C. H. Bryant and P. H. Keesom, Phys. Rev. Letters 4, 460 (1960).
2. H. A. Boorse, A. J. Herschfield and H. Leupold, Phys. Rev. Letters 5, 246 (1960).
3. J. Bardeen, L. N. Cooper, J. R. Schrieffer, Phys. Rev. 108, 1175 (1957).
4. B. L. Chandrasekhar and J. A. Rayne, Phys. Rev. Letters 6, 3 (1961).
5. G. A. Ahlers and D. L. Waldorf, Phys. Rev. Letters 6, 677 (1961).
6. W. H. Keesom and H. Onnes, Leiden Comm. 1924, 174b.
7. M. K. Wilkinson, C. G. Shull, L. D. Roberts and S. Bernstein, Phys. Rev. 97, 889 (1955).
8. A. D. B. Woods and B. N. Brockhouse, Bull. Am. Phys. Soc. 7, 63 (1962).
9. W. K. Weidemann, P. Kienle, and F. Pobelle, Zeit. Phys. 166, 109 (1962).
10. M. Yaqub and C. Hohemenser, Phys. Rev. Letters 9, A4 (1962).
11. G. V. Chester, Phys. Rev. 104, 883 (1956).
12. P. M. Marcus and E. Maxwell, Phys. Rev. 91, 1035 (1953).
13. N. E. Phillips, Phys. Rev. 114, 676 (1959).
14. W. K. Lien (Ph. D. Thesis), University of California (1962).
15. N. Kurti, Cryogenics, 1, 2 (1960).
16. J. M. Daniels and F. N. K. Robinson, Phil. Mag. 44, 630 (1953).

17. J. M. Daniels, Proc. Phys. Soc. (London) A66, 673 (1953).

18. R. A. Erikson, L. D. Roberts and J. W. T. Dabbs, Rev. Sci. Instr. 25, 1178 (1954).

19. N. E. Phillips (Department of Chemistry, University of California, Berkeley), Private communication.

20. G. A. Alers and J. R. Neighbors, Revs. Mod. Phys. 31, 675 (1959).

21. D. D. Betts, A. B. Bhatia, and M. Wyman, Phys. Rev. 104, 37 (1956).

22. T. H. K. Barron, W. T. Berg and J. A. Morrison, Proc. Phys. Soc. 242, 478 (1957); and W. T. Berg and J. A. Morrison, ibid., p. 467.

23. C. A. Bryant and P. H. Keesom, Phys. Rev. 123, 491 (1961).

24. D. Shoenberg, Superconductivity (Cambridge University Press London, 1960), p. 34.

25. W. D. Knight and A. G. Berger, Ann. Phys. 8, 173 (1959).

26. L. C. Hebel, Phys. Rev. 111, 79 (1959).

27. D. Shoenberg, op. cit., p. 66.

28. D. K. Finnemore and D. E. Mapather (Department of Physics, University of Illinois), Private communication.

29. W. S. Corak and C. B. Satterthwaite, Phys. Rev. 102, 662 (1959).

30. J. A. Rayne and B. S. Chandrasekhar, Phys. Rev. 120, 1658 (1960).

31. W. W. Simmons and C. P. Slichter, Phys. Rev. 121, 1580 (1961).

32. R. R. Hewitt and W. D. Knight, Phys. Rev. Letters 3, 18 (1959).

33. R. A. Ferrell, Phys. Rev. Letters 6, 541 (1961).

34. J. G. Daunt and J. L. Olsen, Phys. Rev. Letters, 6, 267 (1961).

35. N. Senozan and N. E. Phillips (Department of Chemistry, University of California), Private communication.

36. F. J. du Chatenier and J. de Nobel, Physica, 28, 181 (1962).

37. J. E. Zimmerman and H. Sato, J. Phys. Chem. Solids, 21, 71 (1961).

38. K. Dransfeld (Department of Physics, University of California), Private communication.

This report was prepared as an account of Government sponsored work. Neither the United States, nor the Commission, nor any person acting on behalf of the Commission:

A. Makes any warranty or representation, expressed or implied, with respect to the accuracy, completeness, or usefulness of the information contained in this report, or that the use of any information, apparatus, method, or process disclosed in this report may not infringe privately owned rights; or

B. Assumes any liabilities with respect to the use of, or for damages resulting from the use of any information, apparatus, method, or process disclosed in this report.

As used in the above, "person acting on behalf of the Commission" includes any employee or contractor of the Commission, or employee of such contractor, to the extent that such employee or contractor of the Commission, or employee of such contractor prepares, disseminates, or provides access to, any information pursuant to his employment or contract with the Commission, or his employment with such contractor.